Universidade de Aveiro
2014

Departamento de Engenharia de Materiais e Cerâmica

Mikalai Zhuk

Grânulos nanoestruturados para libertação controlada de dexametasona

Nanostructured granules for controlled delivery of dexamethasone

Universidade de Aveiro
2014
Departamento de Engenharia de Materiais e Cerâmica

Mikalai Zhuk

Grânulos nanoestruturados para libertação controlada de dexametasona

Nanostructured granules for controlled delivery of dexamethasone

Dissertação apresentada à Universidade de Aveiro para cumprimento dos requisitos necessários à obtenção do grau de Mestre em Ciência e Engenharia de Materiais, realizada sob a orientação científica da Doutora Maria Elizabete Jorge Vieira Costa, Professora Auxiliar e da Doutora Maria Margarida Tavares Almeida, Professora Auxiliar, ambas do Departamento de Engenharia de Materiais e Cerâmica da Universidade de Aveiro.

Dissertation presented to the University of Aveiro to obtain the Master degree in Materials Science and Engineering, under scientific supervision of Dr. Maria Elizabete Jorge Vieira Costa, Auxiliary Professor and Dr. Maria Margarida Tavares Almeida, Auxiliary Professor, both of the Department of Materials and Ceramics Engineering of the University of Aveiro.

o júri

Presidente

Profª Doutora Ana Margarida Madeira Viegas de Barros Timmons

professora auxiliar do Departamento de Química da Universidade de Aveiro

Profª Doutora Maria Elizabete Jorge Vieira da Costa

professora auxiliar do Departamento de Engenharia Cerâmica e do Vidro da Universidade de Aveiro

Doutora Bárbara Joana Martins Leite Ferreira

bolseira de pós-Doutoramento do Departamento de Química da Universidade de Aveiro

agradecimentos

It would be very hard to write this thesis without the help and support of the kind people around me.

Above all, from all my heart I would like to thank my family: my parents Mikalai Zhuk and Alexandra Zhuk and my sister Dasha for motivating and supporting me throughout my life.

This thesis would not have been possible without the help, patience and support of my supervisors Dr. Elizabete Costa and Dr. Margarida Almeida I cannot find words to express my gratitude to Dr. Ana Barros, for her help, advices and understanding.

My appreciations also go to Marta, Celia, Maria Joao, Ana, mr. Jacinto and all people from the department who helped me during my work.

I would like to thank my lab friends Catia, Nathalie, Manuela, Alicia, Rui, Priscila, who made me feel welcome, guided me around the department and showed me Portuguese student traditions.

Thank you my FAME-mates Kyle and Hugues for our trips, nice dinners and time at the ocean.

I would like to appreciate EMMI consortium for holding FAME program and the European Commission for financing my study through Erasmus Mundus Scholarship.

palavras-chave

Sistema de libertação de fármacos, Hidroxiapatite, Quitosano, Dexametasona, Glutaraldeído, Atomização, Estrutura Core-Shell, Modelo Peppas-Sahlin, Modelo Weibull

resumo

Um sistema de libertação de fármacos (DDS) pode transportar de forma precisa o fármaco para o sítio alvo,,i.e., directamente para a zona patológica ou ser administrado localmente. Uma vez no local de interesse, o DDS deve libertar o fármaco de forma controlada, de acordo com as necessidades específicas do paciente, garantindo *in situ* o tratamento desejado, sem efeitos nocivos sobre os tecidos saudáveis.

A parte inorgânica do osso humano é composta principalmente por hidroxiapatite ($Ca_{10}(PO_4)_6(OH)_2$) (HAP). O quitosano (CH), um polímero natural e abundante. Para além de altamente biocompatíveis estes dois compostos são biodegradáveis, podendo ser utilizados em várias aplicações biomédicas (DDS, engenharia de tecidos, implantes, etc.). Além disso, as características de anfifilicidade e as boas propriedades mucoadesivas do quitosano, somadas à capacidade da HAP para absorver diferentes espécies químicas fazem destes compostos materiais desafiantes para um projecto de DDS. O presente trabalho aborda a combinação de HAP com CH para produção de um DDS. A dexametasona (DEX), que é um corticosteróide com acção anti-inflamatória, anti-neoplásica e efeitos imunossupressores, foi o fármaco modelo seleccionado.

Neste trabalho produziram-se grânulos compósitos, com diferentes proporções de HAP e CH, por atomização de suspensões aquosas de HAP, quitosano e DEX. Utilizou-se glutaraldeído (GA) para reticular o CH e procedeu-se também à dupla atomização dos grânulos, uma técnica ainda não reportada na literatura. Os ensaios de libertação do fármaco foram efectuados por imersão dos grânulos carregadas com DEX em solução de fosfato tampão mantida a 37 ° C e sob agitação constante. Alíquotas de PBS foram retiradas após diferentes períodos de tempo e a sua concentração de fármaco avaliada por UV-Vis a λ = 241,5 nm. As características morfológicas e a composição de fases cristalinas dos grânulos atomizados foram avaliadas por micróscopia eletrónica de varrimento (SEM), por adsorção de N_2 usando a isotérmica de BET e por difração de raios-X (XRD). Os resultados obtidos mostraram que a variação da razão (HAP / CH) afectou a morfologia dos grânulos: quando a razão aumenta a morfologia dos grânulos evolui de esférica e rugosa para lisa e com concavidades. Por outro lado as características morfológicas dos grânulos duplamente atomizados indicam uma estrutura *core-shell*.

No que se refere aos resultados de libertação de DEX, verificou-se que grânulos de composição diferente evidenciam perfis de libertação distintos: os grânulos reticulados com GA (0,2 %) apresentam uma curva de libertação mais lenta do que a observada para os grânulos com igual razão HAP/CH mas não modificados; quanto aos grânulos com dupla atomização, estes apresentam um padrão de libertação característico, com duplo patamar, em linha com a referida estrutura core-shell.

Na tentativa de elucidar os mecanismos subjacentes à libertação de DEX, compararam-se os perfis medidos com diferentes modelos matemáticos. Verificou-se que o padrão de libertação da DEX pode ser adequadamente descrito pela equação de Peppas-Sahlin e de Weibull. Em conclusão, a reticulação e a engenharia de morfologia (estrutura *core-shell*) pela via da dupla atomização permitiram melhorar o perfil de libertação de DEX do DDS à base de grânulos compósitos de HAP/CH.

keywords

Drug Delivery System, Hydroxyapatite, Chitosan, Dexamethasone, Glutaraldehyde, Spray Drying, Core-Shell Structure, Drug Release, Peppas-Sahlin Model, Weibull Model

abstract

A Drug Delivery System (DDS) may provide the precise transportation of the medical drug inside the patient's body, directly to the pathological area or alternatively it may be also locally administrated. Once at the site of interest, the ideal DDS is expected to release the drug in a sustained manner according to the specific needs of the patient. As compared to other routes of drug administration, an appropriately designed DDS which active components are conveniently targeted should also ensure the desired in situ treatment without harmful effects of the drug over healthy tissues.

The inorganic part of the human bone is mainly composed by hydroxyapatite ($Ca_{10}(PO_4)_6(OH)_2$) (HAP). Chitosan (CH), a natural polymer, is a linear glucose based polysaccharide. These two compounds are non-toxic, biodegradable and highly biocompatible and hence widely used for various biomedical applications (DDS, tissue engineering, implants, etc.). Moreover, some unique features including the amphiphilicity and good mucoadhesive properties of chitosan together with the ability of HAP to adsorb and then release different chemical species make these compounds challenging materials for DDS design. The present work addresses the combination of HAP and CH with a drug model aimed at engineering a DDS with a controlled drug release. Dexamethasone (DEX) is the drug model here selected. DEX is a corticosteroid with anti-inflammatory, antineoplastic and immunosuppressant effects, which is used for the treatment of various diseases like endocrine, dermatologic and neoplastic disorders and cancer among others.

In the present research, composite granules with different ratios of HAP and CH components were produced by spray drying aqueous suspension of HAP, chitosan and DEX. To reduce polymer swelling, Glutaraldehyde (GA) was used to cross-link CH. Granules were also produced by a double spray drying technique, which so far has not been yet reported in the literature.

The morphology and crystal phase composition of the produced granules were evaluated by scanning electron microscopy (SEM), N_2 adsorption using the BET isotherm (BET), and X-ray diffraction (XRD). The obtained results showed that the variation of (HAP/CH) ratio affected the morphology of the granules as when that ratio increases the granules morphology changes from spherical with rough surface to a shape with concavities and smooth surface. Regarding the granules obtained by double spray drying, their morphological characteristics indicated that a core-shell structure was obtained.

The drug release experiments were carried out by immersing the DEX loaded granules into phosphate buffer solution (PBS), kept at 37 °C under constant stirring. Aliquots of PBS were withdrawn after different times and their drug content evaluated by UV-Vis spectroscopy at λ= 241,5 nm. The results showed that granules with different composition could display different drug release patterns: HAP/CH granules cross-linked with GA (0,2 wt %) exhibit a more sustained drug release than granules with the same HAP/CH ratio without modification; as for double spray dried granules, a characteristic profile with a double plateau was observed, in line with a core-shell structure.

Attempting to elucidate the mechanisms underlying DEX release, different mathematical models were compared with the measured release profiles. It was found that Peppas-Sahlin and Weibull equations are appropriate models for predicting the drug release from the produced granules. In conclusion, the cross-linking and morphology engineering (core-shell structure) via double spray drying allowed improving DEX release profile of HAP/CH DDSs.

LIST OF CONTENTS

LIST OF FIGURES

LIST OF TABLES

ABBREVIATIONS

BET – Brunauer–Emmett–Teller method

CH – Chitosan

DD – Degree of Deacetylation

DDS – Drug Delivery System

DEX – Dexamethasone

DMF – Dimethylformamide

DMSO – Dimethyl sulfoxide

DPV – Differential Pulse Voltammetry

FLIM – Fluorescence Lifetime Imaging Microscopy

FTIR – Fourier Transform Infrared Spectroscopy

GA – Glutaraldehyde

HAP – Hydroxyapatite

PBS – Phosphate buffered saline

SEM – Scanning Electron Microscopy

SW-AdsV – Square - wave adsorptive voltammetry

UV-vis – Ultraviolet–visible spectroscopy

XRD – X-Ray Diffraction

GLOSSARY

Angiogenesis	–	The physiological process of formation of new blood vessels in an organ or tissue
Biocompatibility	–	The ability of a material, integrated into the patient's body, to perform its desired functions without causing harmful effects.
Bioresorbability	–	The ability to be broken down and be absorbed by the body, without the need to be remove.
Deacetylation	–	The process of acetyl groups removal from an organic compound
In vitro	–	In experimental biology refers to research taking place in glass/plastic container in a laboratory (outside a living body)
In vivo	–	In experimental biology refers to study in a living organism (opposite to in vitro)
Osteoconductivity	–	Property of a material that encourages bone growing on its surface
Osteogenesis	–	A process of a new bone development and formation

Chapter 1

Introduction and Objectives

1. Introduction

One of the main ideas of the pharmacotherapy is to impact the affected part of the organism with a minimal negative effect to the whole body. A big number of drugs, like antibiotics, steroids, et al. can be dangerous if used in high dosages. The routes of medicines administration can be divided in four groups: enteral (delivered through the digestive tract), parenteral (bypassing the digestive system), topical (through the skin) and inhalation (via the respiratory tract). Different routes provide the possibility of regulating localisation, duration and velocity of medical effect. For example, the same drug substance taken orally or with an injection will start to impact in 2 − 4 hours or 10 − 20 minutes respectively. A big disadvantage of the most peroral medication is the wide dissemination of the active components around the body. As a result higher dosages should be used to achieve the required therapeutic effect. The other limitations are that oral drugs can irritate the gastric mucosa or some of them can be decomposed by gastric juice. Since oral administrations, like all the enteral routes, have mainly a systemic action, the drug will also affect the uninjured parts of the body. However, the enteral administration is the most common in pharmaceutical therapy, due to its simplicity and the unassisted way of the method.

The idea of the drug delivery systems (DDS) is the achievement of the required therapeutic effect. Such systems provide the precise transportation of the medicine inside the patient's body directly to the pathological area, e.g. the injured organ or the nidus of inflammation. Due to their local application, DDS make it possible to use lower drug dosages. Properly chosen DDS with the controlled drug release allow having the prescribed concentration of the medicament during the therapy. Among all the other routes of medicine administration DDS is the most local and accurate way of medical treatment. The precise localisation of the active components minimizes the harmful effect.

In recent years the number of studies of the DDS has increased rapidly. Currently many new systems are under medical testing. Depending on the properties of a drug substance, localization and type of disease different materials can be used as a drug carrier. There are systems based on polymers, lipids, protein/peptide nanotubes, metal nanostructures, composites, etc. (1).

Drug delivery systems provide a wide range of applications. One of the most perspective is the treatment of the different kinds of cancer. However, limited number of DDS at the pharmaceutical market is determined by the necessity of deep and precise analyses. The possible side effects of many DDS, as new medical substances, are still under on-going research.

Design and construction of a new DDS requires approximately $ 20 – 50 million and 3 – 5 years of work, sometimes clinical research can increase the time and final outlays. The world market of DDS shows continuous growth (Figure 1), thus in 2016 it should overcome $ 175 billion per year. The global market for drug delivery systems in 2010 was $ 131,6 billion (59 % contributed by the USA, 27 % – Europe, 14 % – the rest of the world) (2).

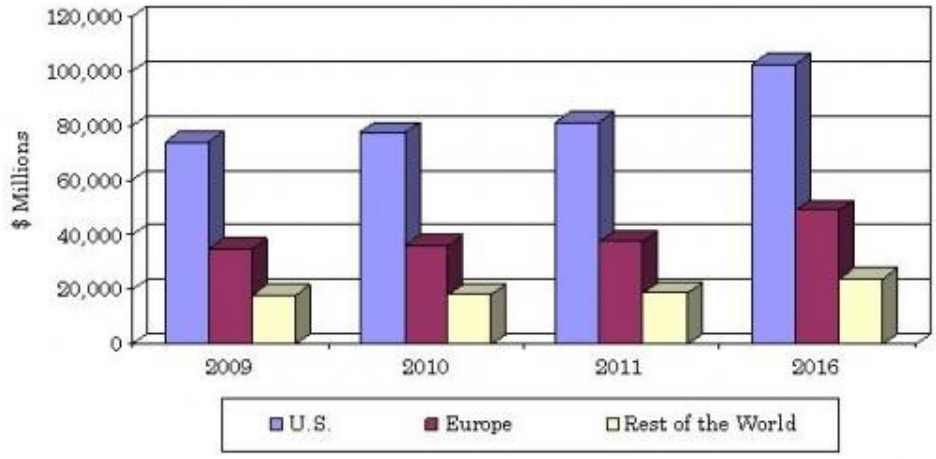

Figure 1 – Global revenue of advanced drug delivery systems 2009 – 2016 (2).

For aging people the increase of such bone diseases as osteoporosis, osteoarthritis and bone cancer is a serious problem. Osteoporosis (the disease of decreasing bone mass and density) is the reason of more than 1,3 million bone fractures each year. Especially hip and spine fractures are the most dangerous and harmful for patients. Very often bone disease becomes chronic and requires a long-term pharmacological therapy. Since bones are distributes throughout the body there are difficulties to maintain required concentration of the drug. Moreover, toxic-therapeutic window for bone treatment is usually narrow (3).

Designing a good DDS for bone treatment the following obstacles should be taken into account:

- Drug carriers with large diameter (as liposomes for example) are not suitable for bone DDS, since the accessibility of large elements to the bone surface is limited. Bones possess membrane of lining cells, which functions as a marrow-blood barrier.
- Bone mainly consists of mineral hydroxyapatite.
- The efficiency of biomolecules with specific targeting affinity (e.g. enzymes, antigens) may be very low in mineralised surrounding (3).

If a second surgery is not needed it is desirable for implanted devices to be removed device after all the drug has been released. Thus the application of bioresorbable material to design DDS for bone treatment is preferable (4).

1.1. Objectives

The main objective of this research is to develop a drug delivery system based on hydroxyapatite/chitosan particles, study the mechanisms underlying the DDS and compare different mathematical models for drug release prediction.

1.2. Thesis structure

This report consists of five chapters. Chapter 1 addresses the interest and objectives of the present study. There is a literature review about drug delivery systems, dwelling on drug delivery systems, applied requirements to them, materials the DDS are made from and techniques of their manufacture in Chapter 2. The problem formulation of this research is presented in Chapter 3. Chapter 4 describes materials and methods of the experimental procedure. The results and discussions are presented in Chapter 5. Finally the main conclusions and recommendations are summarized in Chapter 6.

Chapter 2

Literature review

2. Literature review

2.1. Drug Delivery Systems (DDS)

With the recent developments of medicine the old drug dosage forms became unsatisfactory to face the new challenging needs. The novel treatment approaches required new drug carriers, which could maintain a steady release of drug to the specific site of action. Therefore, drug delivery systems (DDSs) were developed. The first DDS originated in late 1930s, with a presentation at the Royal Society of medicine in London made by R. Deansby and A.S. Parkes. Their work was about sustained release of estrogen in several animals (5).

Figure 2 illustrates the advantage of controlled drug release, which allows achieving a therapeutic effect in human body for a required time. Controlled released allows to obtain a more stable and predictable concentration of the drug in the organism within the therapeutic range. A DDS as opposed to one dosage of drug administration eliminates toxic concentrations. For an appropriate medical treatment the concentration of the drug should be maintained above ineffective, but below toxic level.

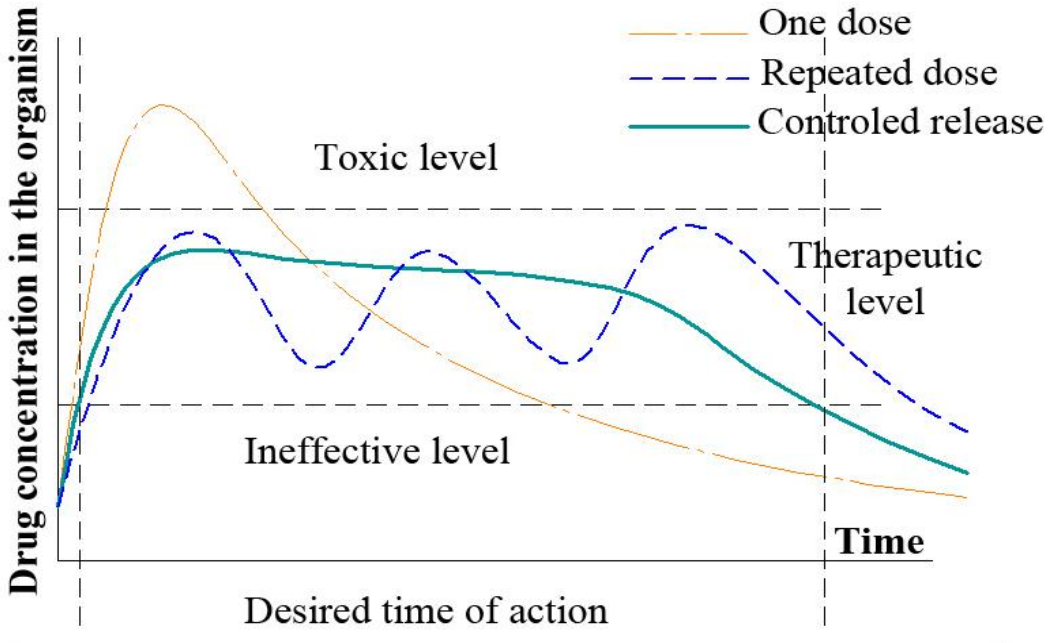

Figure 2 – A schematic drawing illustrating the controlled drug release(adapted from (6)).

K.K. Jain (4) summarized the characteristics of an ideal drug delivery system as follows:

- It should increase the bioavailability of the drug.
- It should provide for controlled drug delivery.
- It should transport the drug intact to the site of action while avoiding the nondiseased host tissues.
- The product should be stable and delivery should be maintained under various physiological variables.
- A high degree of drug dispersion.
- It should be easy to administer to the patients.
- It should be safe and reliable.
- It should be cost-effective.

While the ideal DDS is a goal to be pursued, the real DDSs are known to offer significant advantages over traditional systems though some disadvantages are still to be solved. Table 1 sums up the advantages and disadvantages of DDSs over traditional systems.

Table 1 – Advantages and disadvantages of DDSs.

Advantages of DDS	**DDS disadvantages**
Maintenance of optimal concentration of drug.	Possibility of toxicity of the materials.
Ability to deliver a drug selectively to a specific area.	Harmful degradation products.
Improving efficacy with less amount of drug	Necessity of surgical intervention either on systems application or removal.
Minimization of side effects.	Patients discomfort with DDS device usage.
Less frequent drug dosing.	High cost of final product.

According to literature Drug delivery systems can be divided in two main groups: time ***controlled (sustained)*** and ***spatially controlled (targeted)*** (3).

Nanoparticles systems can improve the efficacy of drug delivery. One of the main advantages of nanoparticles is their large surface area. Nanoparticles tend to improve the efficiency and bioavailability of the drug by encapsulating high amount of medicine. The other outstanding advantage is the possibility of various modification of nanoparticle surface, which can be used for specific targeting to a tissue or cell for example (7).

Several types of nanoparticle-based DDSs are presented in Figure 3, i.e liposomes, dendrimers, ligands, magnetic particles. Most of these DDSs can be attributed to the ***targeted DDS***.

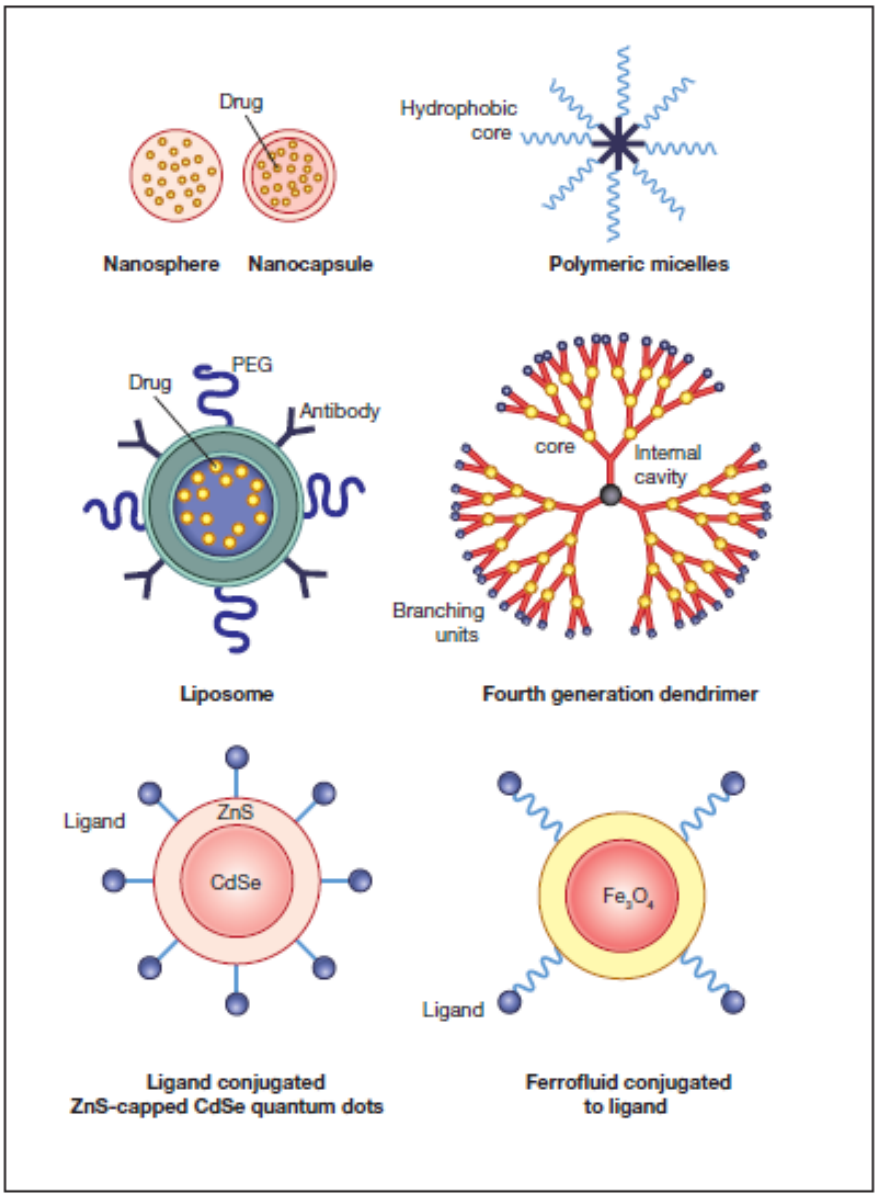

Figure 3 – Different types of nanotechnology-based drug delivery systems (8).

In the case of polymeric micelles the therapeutic agent is loaded into the core, which is surrounded by copolymers forming an outer hydrophilic layer. The outer layer controls *in vivo* behaviour of DDS and the inner core of micelle structure responsible for drug loading (9). For example Wei Xu in (10) discussed application of polymeric micelles to protect poorly water-soluble drugs from gastrointestinal environment for controllable drug release in oral administration. Nowadays polymeric micelles system DDS becomes important for tumour diagnosis and therapy (9).

The advantage of liposomes is that their surface can be modified with various targeting ligands and attaching polyethylene glycol (PEG) units, which allows to get the so called “stealth liposome”. Stealth liposomes, due to their ability to avoid detection of an immune system, can circulate in the bloodstream during a prolonged time (8). The liposomes based DDS have been studied for the last 50 years. Liposomes are most commonly used as vehicles for drugs and antibodies targeted for the delivery of anticancer agents. Liposome DDSs allow to deliver various types of drugs, among which the following ones can be mentioned: anesthetics and anti-inflammatory drugs; the delivery of gene medicines; anti-cancer, anti-fungal and antibiotic drugs delivery (11).

A large number of functionalizable groups make dendrimers very appropriate candidates for DDSs. Dendrimers are three-dimensional symmetric macromolecules. The tree- like structure of the reactive end groups of dendrimers are built around a central internal cavity molecule. Dendrimers-based DDSs are often used as chemotherapeutic agents for the treatment of cancer (8). Tailor-made surface of dendrimers allows wide opportunities for construction and tuning DDS with outstanding characteristics. Thus, Menjoge *et al.* studied dendrimers systems able to transport drug across human placenta, which opens a good perspectives for treatment selective treatment of pregnant women with minimizing harmful effect of the drug for the foetus (12-13).

Quantum dots are nanosized (1-10nm) semiconductors crystals able to fluorescence. Quantum dots provide a new class of nanosystems for cells/tumour labelling. Quantum dots cannot be used as a drug carrier, but their usage in combined DDSs enhances the diagnosis of tumour in cancer treatment (8). Figure 4 illustrates quantum dots application for tumour imaging (14).

Application of ferrofluids (colloidal solutions of iron oxide magnetic nanoparticles surrounded by a polymeric layer) in DDSs for example provides control of drug release by an external magnetic field (4,8). The same as quantum dots magnetic nanoparticle can be used in combined and complex structured DDSs. It was reported that magnetic nanoparticles DDSs have promising potential in gene therapy (15).

The DDSs that allows achieving prolonged therapeutic effect by continuously drug releasing during a prolonged time after administration are called ***sustained DDSs*** . This type of DDS is designed to reduce dosing frequency and to increase the effectiveness of medicines thanks to drug localization (16).

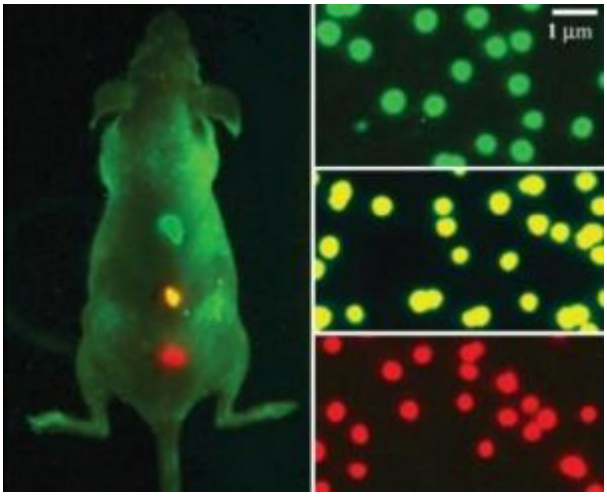

Figure 4 – Tumour imaging in live animal **(14)**.

To get the maximal local drug delivery, the drug carriers should be able to contain a maximal amount of the drug. From this viewpoint, the advantage of using granules and porous materials, having high surface area, becomes obvious. Microspheres as DDSs can be used for a great number of applications: chemotherapy, cardiovascular disease therapy, hormone therapy, therapeutic protein delivery and vaccine development (17). Many of microspheres DDSs are sustained systems.

Microspheres DDSs are presented by approximately spherical particles with the size in a range from 1 to 1000 µm. Microcapsules are the form of microsphere DDS (Figure 5). The difference of these systems is in drug location, thus microsphere represents matrix system with drug entrapped across it whole volume. In microcapsules drug is inside the system and the outer layer is presented by polymer coat. As it is seen from Figure 5 microcapsules can be different than spherical geometry (18).

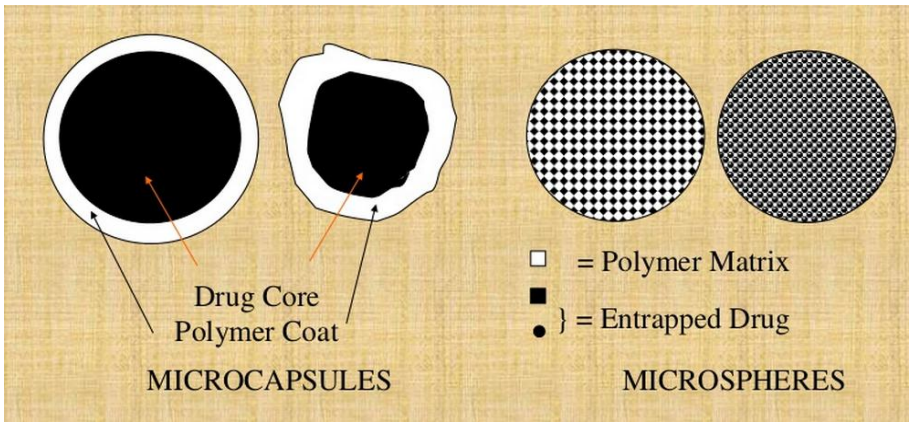

Figure 5 – Structure of Microcapsules and microspheres used for drug delivery **(18)**.

One of the most common materials for microspheres production are: biodegradable polymers (Chitosan, Alginic acid, Polyesters, etc.) (19). However, non-biodegradable polymers for different application can be used (Glycidyl methacrylate, Acrolein, etc.) (18). For bone treatment hydroxyapatite (HAP) microspheres are used. (20) Figure 6 presents microstructured HAP microspheres produced by solid-in-water-in-oil (S/W/O) and studied by M.C. Sunny *et.al.* In his work M.C. Sunny used Chitosan (CH) as a binder for small HAP particles to form microspheres of desired size (20).

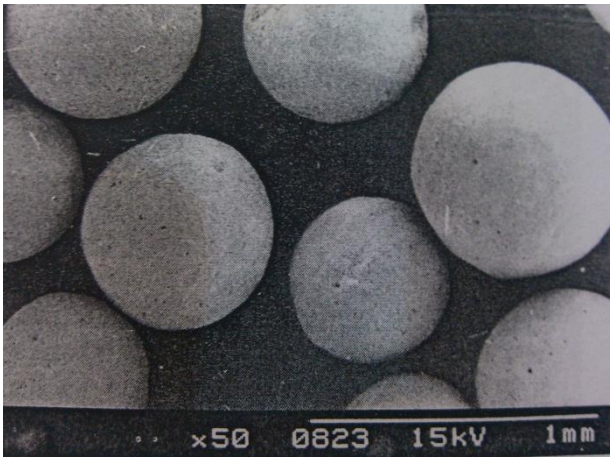

Figure 6 – HAP-Chitosan microspheres **(20)**.

In the following paragraphs the methods of microsphere production and drug loading will be presented.

2.1.1. Drug loading

In general all the drug loading methods can be divided in two groups:

- ***Incorporation methods*** – loading during the preparation of the particles (spray drying, freeze-drying, etc.).
- ***Incubation methods*** – loading after the formation of the particles (soaking technique, vacuum adsorption, etc.) (21).

The maximal drug loading can be achieved by incorporation methods (21). However, during spray drying the drug from the solution will be stored in the carriers in solid form. As a result the release will be more rapid as compared to the release when the drug is absorbed on the particles surface. All the appropriate techniques of the granule synthesis (spray drying, freeze-drying,) can be applied for the incorporation of the drug loading. The drug solution should be used as one of the initial components before the formation of the granules.

One of the simplest ways of incorporating the drug into the carrier is the soaking technique. When applying this method, the carriers are placed into the drug solution for a certain time, during which the drug is being absorbed from the solution. The drug content can be enhanced by increasing the drug concentration and the soaking time. The Vacuum adsorption is a more advanced method. The promotion of the drug adsorption is achieved by the initial location of the particles into the medium with reduced pressure. Thus, after the carriers are put into the solution, the adsorption goes faster (21).

2.1.2. Drug release mechanisms

The drug release from the chitosan carrier includes three processes; shown on Figure 7; (release from the surface, diffusion from the swollen matrix, release due to erosion) Usually the release from the DDS cannot be described by only one process but in a varying degree by a combination of the processes shown on Figure 7. The more rapid process is the release from the particle surface, when the absorbed drug instantaneously dissolves in the surrounding medium. Such burst release was observed by He *at al*. (22) in their research chitosan granules loaded with different drugs (cimetidine, famotidine or nizatidine) were studied. It was shown that cross linking can reduce burst release.

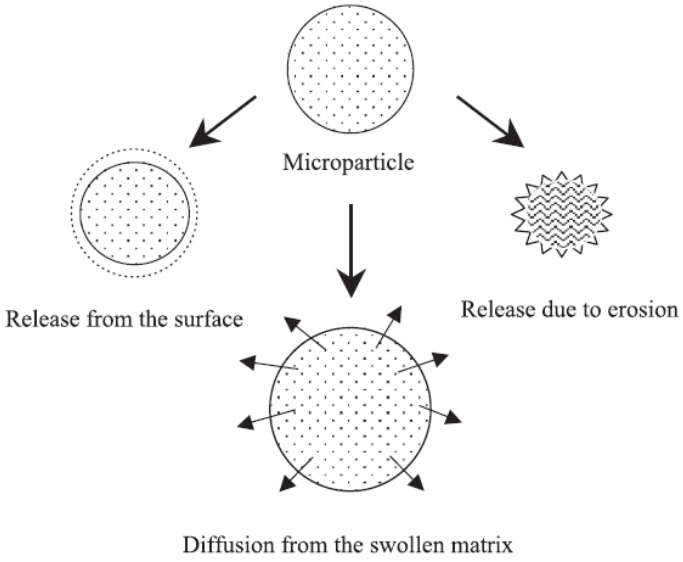

Figure 7 – Drug release from the micro particle (21).

Drug release by diffusion is divided on three following steps:

1. Water penetrates into particle, which starts swelling of polymer;
2. Conversion polymer from glassy into rubbery state;
3. Drug diffusion from swollen rubbery polymer (21).

It should be mentioned that for CH with higher molecular wait the release of a drug is slower, what can be explained by lower solubility and higher viscosity of high molecular weight CH in compare with low molecular weight CH (21).

2.1.3. Modelling the drug release

With the application of mathematical modelling it is possible to predict the release kinetics of the DDS, which is useful for the optimization of its design. Selecting the appropriate kinetic model for the drug delivery system is important for the identification of the parameters influencing the drug release. The methods used for studying the kinetics of the drug release can be divided into three groups (23):

- Statistical methods (exploratory data analysis method, repeated measures design, multivariate approach, etc.);
- Model based methods (zero order, first order, Higuchi, Korsmeyer-Peppas model, Hixson Crowell, Baker-Lonsdale model and Weibull model among others);
- Model independent methods.

In the present work Statistical methods and Model independent methods will not be discussed. The first due to its complexity. The second due to some limitations introduced by two factors (difference factor (f1) and a similarity factor (f2)) used in this method, which are sensitive to the number of dissolution points (23).

Regarding model based methods, the main features of the most cited models will be reviewed in the next paragraphs.

Higuchi model was the first mathematical model proposed in 1961 to describe the drug release for planar systems. Later it was generalised and adapted for different types of DDSs by the other scientists (23).The original equation has the view of Equation 1 (24-25).

$$\frac{M_t}{A} = \sqrt{D(2c_0 - c_s)c_s t} \qquad \text{for} \quad c_0 > c_s \tag{1}$$

Where: M_t is amount of the drug released for the time t; A is surface area of the drug carrier; D is the diffusion coefficient of the drug; c_0 and c_s are the initial concentration of the drug and the solubility of the drug in the matrix. Equation 1 can be simplified to the Equation 2:

$$\frac{M_t}{M_0} = K\sqrt{t} \tag{2}$$

Where: M_0 is the total amount of the drug at time t=0 and K is the release rate constant showing the design variables of the DDS (geometry of the system: size, shape and

porosity of the carrier). The advantage of this model is in its simplicity: the amount of the drug released is proportional to the square root of the time. Nevertheless, before using Higuchi model the following assumptions should be considered:

- the initial concentration of the drug should be higher than its solubility ($c_0 > c_s$);
- the drug diffusion takes place in one dimension;
- the diameter of the drug particles should be much smaller than the thickness of the system;
- the swelling and dissolution of the matrix is negligible;
- the diffusion of the drug is constant (24-26).

Due to its simplicity Higuchi model can be applied for some systems to describe the release process in general. However, to attain more accurate results other kinetics models should be used. For the spherical matrix it is possible to apply the Baker–Lonsdale model (Equation 3), which was obtained from the Higuchi model.

$$\frac{3}{2}\left[1-\left(1-\frac{M_t}{M_0}\right)^{2/3}\right]-\frac{M_t}{M_0}=\frac{3Dc_s}{r_0^2c_0}t \quad (3)$$

It is obvious that Equation 3 represents a more specific system than the “general” Higuchi model. Thus, the impact of the spherical matrix radius r_0 is already considered. Moreover, if the system is not homogeneous and has porosity or fractures the Baker–Lonsdale model can be enhanced (Seki et al). (Equation 4) (26).

$$\frac{3}{2}\left[1-\left(1-\frac{M_t}{M_0}\right)^{2/3}\right]-\frac{M_t}{M_0}=\frac{3Dc_s\varepsilon}{r_0^2c_0\tau}t \quad (4)$$

Where ε is the porosity of the matrix and τ is the tortuosity factor of the capillary system.

Mathematical models help to optimize the interpretation and description of the drug release profile. Sometimes a big number of parameters and different physical and chemical mechanisms can influence the kinetic release, which makes it difficult or even impossible to obtain exact mathematical model. For a more general description of the drug release process Higuchi model, zero order model, Weibull model and Korsmeyer–Peppas model can be used. (26)

The ***zero order*** model is applied for the matrix tablets with low soluble drugs, osmotic systems, some transdermal systems, coated dosage forms and membrane systems. Zero order release kinetics is typical for the following types of drugs: heart and blood pressure maintenances, pain controllers, antidepressants, etc. (27)

The **Hixson-Crowell** (Equation 5) model has several assumptions:

- The geometry of the particles is considered to be spherical and doesn't change with time
- The particles remain intact and do not disintegrate into smaller fragments during dissolution

For spherical geometry, the mathematical equation for this model is written as follows

$$\frac{\mathrm{M_t}}{\mathrm{M_0}} = 1 - \left(1 - \frac{k_{er,0} \cdot t}{C_0 \cdot R}\right)^3 \quad (5)$$

The **Weibull** Equation 6 defines the cumulative fractional drug release expression as a function of time as follows:

$$\frac{\mathrm{M_t}}{\mathrm{M_0}} = 1 - \exp\left(\frac{-\left(t - t_{lag}\right)^b}{t_{scale}}\right) \quad (6)$$

Because Weibull model is an empiric, it is criticized, since presents some deficiencies :

- There is not any kinetic fundament and could only describe, but does not adequately characterize, the dissolution kinetic properties of the drug;
- there is not any single parameter related with the intrinsic dissolution rate of the drug;
- it is of limited use for establishing in vivo/in vitro correlations.

Mathematical modelling has significant role in elucidating the important drug release mechanisms in DDSs. The transportation of drug inside DDS involves various physical and chemical phenomenon, making it difficult or sometimes even impossible to get the appropriate mathematical model for correct drug release description. Almost all mathematical models correspond to the known release mechanisms (diffusion-, swelling-, and erosion-controlled) (28).

2.2. Hydroxyapatite

2.2.1. General information about hydroxyapatite (HAP)

The human skeleton contains 20% of trabecular bone and 80% of cortical bone. Trabecular (cancellous) bone has a high porosity (50–90%) while cortical bone is a compact type of bone with 10 % porosity.

The Human bone is a porous composite composed of an organic component (collagen) and an inorganic component (calcium phosphate, mainly in hydroxyapatite (HAP) form).The bone composition includes 60% of inorganic phase (mineral phase), 30% of organic matter, and 10% of water. The inorganic part is mainly represented by HAP. HAP crystals are small plates 2-3nm thick and tens of nanometres in length and width that precipitate onto the collagen fibres.

The interaction between bone chemical components explains its unique mechanical properties, in which the compressive strength is originated from the rigid HAP, while collagen fibrils are capable of energy dissipation and impart the tensile properties. The Figure 8 illustrates the complex structure of the human bone (29).

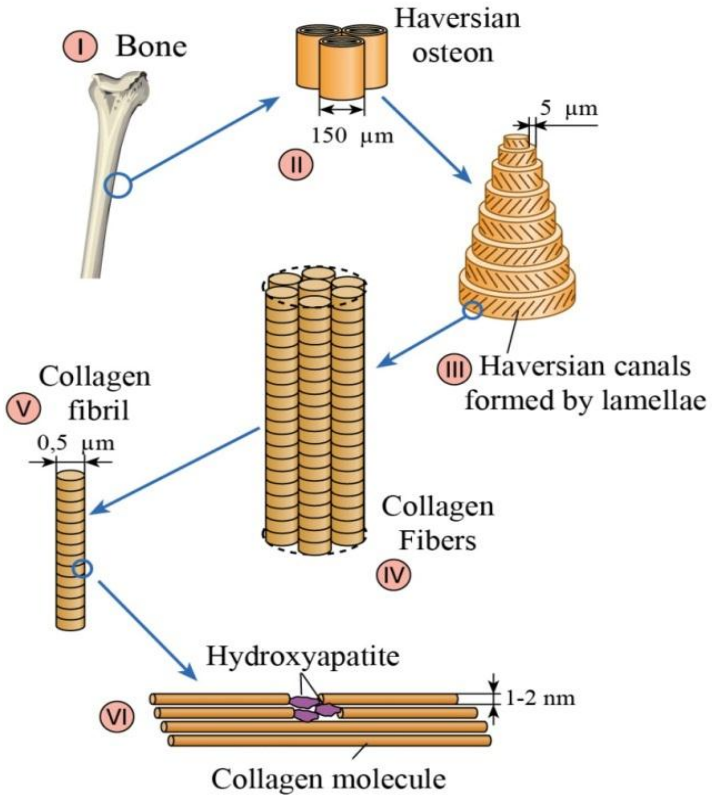

Figure 8 – Structure of human bone.

Hydroxyapatite ($Ca_{10}(PO_4)_6(OH)_2$) (HAP) based materials are widely used for biomedical applications, due to their chemical and structural similarity to the natural bone. In addition hydroxyapatite is a bioactive, biocompatible, bioresorbable and osteoconductive material with a good bone integration ability. HAP has been under study for the last sixty years and has been used in calcium phosphate cements, scaffolds for bone and dental replacement surgeries, drug delivery systems (DDS), etc.

Depending on the Ca/P ratio there exist different modifications of calcium phosphates. This ratio can range from 0,5 to 2,0 determining the existence of different stoichiometric calcium phosphates: dicalcium phosphate dihydrate (brushite) – 1,0; octacalcium phosphate (OCP) – 1,33; α-tricalcium phosphate (α-TCP) – 1,5; β-tricalcium phosphate (β-TCP) – 1,5; hydroxyapatite – 1,67; tetracalcium phosphate – 2,0 and others. (30) As compared with HAP, β-TCP is more soluble; HAP has the best thermodynamic stability in physical environment (pH ≥ 5,4) among all the other calcium phosphates. (31)

There is an opinion that the shape of HAP particles has a significant influence on the inflammatory risk. Therefore, the round regular-shaped particles are considered more preferable in comparison with the irregular-shaped ones (31). However, for the nanoscale particles, used for the drug delivery, this assumption can be questioned.

As a drug delivery system (DDS) HAP can be used in the form of nanoparticles, in composite materials with different polymers and as a component of calcium phosphates cements or scaffolds.

2.2.2. Synthesis of HAP

One important objective has been to synthesise HAP as close as possible to the biological apatite. Nowadays it is possible to synthesise hydroxyapatite using various methods; precipitation from solutions, sol-gel method, solid state reactions, hydrothermal processing, electrospraying, flux cooling method, ultrasound and mechanochemical processing, etc. (32). Wet chemical syntheses methods are the cheapest and the simplest. However, among the disadvantages of these methods are the variability of morphology, crystallinity and size of hydroxyapatite particles (30). The final properties of HAP depend significantly on the shape, size, crystallinity and morphology of hydroxyapatite particles. It is possible to reach the required properties by choosing the synthesis technique and by varying its parameters. Thus, the increase of the sintering temperature of the particles synthesized by the sol-gel method, allows increasing the

crystallinity and the crystallite size of the final HAP particles (33). Even a small change of pH during the precipitation method affects significantly the particles' size (34). Plasma spraying is among the most commonly used techniques for the commercial synthesis of HAP (30). The particle size and some advantages/disadvantages of different techniques are compared in the Table 2.

The wet chemical methods (precipitation methods) are cheap and easy routes for HAP synthesis. However they have several drawbacks. Among them there are, first of all, the difficult reproducibility of the particle morphology and crystallinity. Secondly, the size of the particles is different and distributed non-uniformly. Formulas 7 and 8 are two common reaction described hydroxyapatite synthesis by wet chemical route (35):

$$10Ca(NO_3)_2 + 6(NH_4)_2HPO_4 + 8NH_4OH \rightarrow Ca10(PO_4)_6(OH)_2 + 20NH_4NO_3 + 6H_2O \quad (7)$$

$$10Ca(OH)_2 + 6H_3PO_4 \rightarrow Ca_{10}(PO_4)_6(OH)_2 + 18H_2O \quad (8)$$

In the precipitation method the particle morphology and the precipitated calcium phosphate phase depend on the pH during the reaction and on the Ca/P ratio of the reagents. The variation of these parameters can influence the final crystal structure that can be contaminated with different modifications of calcium phosphates (brushite, monetite, etc.) (33).

The sol-gel is a two-phase technique in which the solution is converted to an amorphous gel which is dried afterwards. This method allows synthesising HAP particles of a nanometric size (35). Since the sol-gel technique provides a molecular-level mixing of calcium and phosphorus precursors, the homogeneity of the final HAP is high (33). Among the disadvantages of this method are the impurities and the poor crystallinity of the resulting product (35).

Needle-like form particles with nanometric or micrometric sizes can be obtained using the hydrothermal technique. This method is based on the usage of high pressure and temperature. For example, hydroxyapatite particles can be synthesised by the reaction of calcium carbonate and diammonium hydrogen phosphate at re-crystallisation temperatures (200 – 300 °C) with the pressure of 1 – 2 kbar. Similarly to the previous two techniques, during the hydrothermal method it is difficult to regulate the size of HAP particles (33,35).

Nowadays plasma spraying is the most widespread technique for commercial production of HAP coatings.

Table 2 – Comparison of different synthesis methods of HAP (30).

Method	Particle size	Comments
wet chemical	0,07–0,64 μm	cheap, simple and slow; difficult to regulate particle size
solid-state process	0,1–1 μm	difficult to regulate particle size and multiple phases seen in crystallisation
hydrothermal	1 μm	difficult to regulate particle size
mechanical–chemical	0,13–0,14 μm	simple but process requires strict adherence to recipe
synthesis sol–gel	nanosized	subject to impurities
chemical synthesis	50 nm	subject to impurities
sputter coating	0,5–3 μm	cheap but line of sight technique and high temperatures introduce additional phases
plasma spraying	30–200 μm	uniform coating but surface coating amorphous

2.2.3. HAP applications

HAP has a wide application in scaffolds for bone tissue engineering, due to its bioactivity and osteoconductivity, HAP also induces osteogenesis. A good review of this subject can be found in the paper of K. Fox *et al.* (30) that covers the recent advances of nanophase hydroxyapatite applications.

Recently studies are directed on the possibility of combining HAP with different types of drug and materials for multipurpose applications, which can include cancer therapy, antimicrobial treatments, magnetic manipulation, osteoporosis treatment (30). HAP can be used in the production of nanoparticles, powders (36), drug delivery systems (37).

HAP and related to it calcium phosphates have an excellent ability to bond to bone. Nano-hydrohyapatite is applied for bone augmentation, coating implants, as fillers in bone or teeth (30). The porous HAP-based scaffolds are used for the treatment of bone fractures, tumours and in the replacement of failed or loose joint. When HAP is used as a coating for implants it reduces aseptic loosening by improving bone apposition and osteoconductivity at the implant/bone interface.

In 1970-s it was found that proteins could reversibly adsorb to HAP surface. HAP “history” as a material for drug delivery started can date back to this time. In spite of burst drug release, HAP surface can adsorb different medicaments that together with its compatibility inspired scientists to study HAP as a drug carrier material. HAP due to the negative charge of its core (-13.9 mV) can form a tight attraction with the positively

charged chitosan. This interaction restrained the loaded drug, what is useful for prolonged drug release (30). HAP can be a drug carrier in different forms. The drug can be encapsulated inside HAP microspheres, loaded on the surface of HAP scaffolds or used in calcium phosphate cements (30).

Hap finds its main biomedical applications in scaffolds, dental implants, cements, drug delivery, coatings promoting bone ingrowth, bioactive glasses and etc.

2.2.4. Debates about toxicity

Although HAP has been studied for more than 50 years and used in numerous biomedical applications, there are still some disputes about the toxicity of hydroxyapatite nanoparticles. Thus, there were some ambiguities about cytotoxicity and genotoxicity of HAP nanoparticles. There is an opinion that nanoparticles can agglomerate inside the blood vessels similar to cholesterol. It is known that HAP can promote artery calcification as part of atherosclerosis. Therefore, when using HAP nanoparticles, possible atherosclerotic complications should be kept in mind. However, different clinical tests have not yet showed the real threat of HAP toxicity. Moreover, these nanoparticles were accepted on the US (FDA approval) and the EU (CE mark) markets (30).

2.3. Chitosan

2.3.1. General information about chitosan

Chitosan is a natural linear glucose based polysaccharide. There are two main characteristics that impact chitosan properties: the degree of acetylation and the molecular weight. The deacetylation degree shows the percentage of D-glucosamine in the chitosan molecule. Thus, chitosan with 80% deacetylation degree contains on average 80% of D-glucosamine residues and 20% of N-acetyl-D-glucosamine residues. Chitin is named chitosan in case the deacetylation degree is 60 – 100 % (Figure 9). The acid dissociation constant (pKa) and chitosan solubility can be modified by changing the degree of deacetylation. Due to the loss of charge chitosan will precipitate from the solution at neutral pH (38). It is found that chitosan can improve osteogenesis and angiogenic activity (39). The range of biological properties such as wound healing, osteogenesis enhancement and biodegradation are dependent on the viscosity of the chitosan solution. The viscosity can also be varied by changing the deacetylation degree

(31). Commercial chitosan is obtained from the shells of shrimp and other sea crustaceans.

Chitosan is nontoxic, due to its degradation to the amino sugars, which are harmless and easily removable from the organism (21).

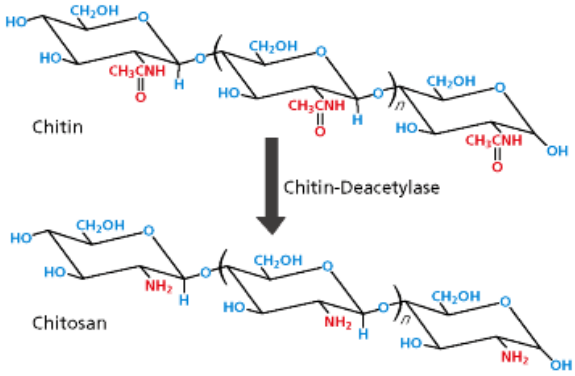

Figure 9 – Chemical structures of chitin and chitosan (40).

Thanks to the primary amino group chitosan has a cationic nature. This fact makes possible the interaction of chitosan with negativly charged surfaces (for example, proteins). As compared to many other natural polymers, chitosan is a unique one that has a positive charge. Due to the above mentioned properties and good mucoadhesive effect, there are numerous drug delivery systems based on chitosan (oral, ocular, nasal, vaginal, buccal, parenteral, intravesical and other DDS). Chitosan (CH) has a few disadvantages, among which are low mechanical properties, chemical and temperature instability (41).

Although there are still a lot of on-going researches, the first DDS products have been already registered at the pharmaceutical market. Ciclopoli® containing a chitosan derivative (hydroxypropyl–chitosan) is one of them (41).

To improve characteristic of chitosan and to decrease its swelling CH should be cross-linked. The crosslinking is formed by the no uniform length of chains and by terminal unities. This process can involve two CH unites of the same or different polymeric chain. In present work Glutaraldehyde (GA) was used as cross-ling agent. GA reacts with primary amine groups, what produces covalent glutaraldehyde crosslinking (42).

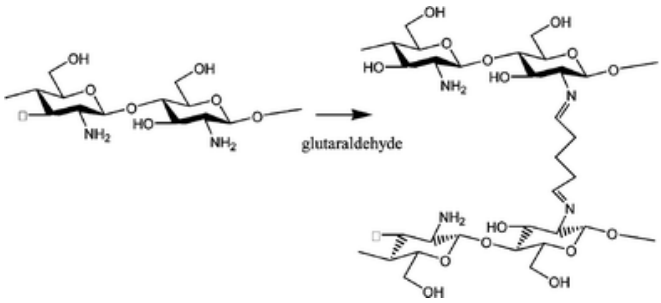

Figure 10 – Crosslinking of chitosan using glutaraldehyde **(43)**.

2.3.2. Methods for granules production

There are several methods for producing CH granules. The ***coacervation/precipitation*** method (Figure 11(a)) is based on the property of chitosan to precipitate in alkaline solution. For the production of the particles the solution of chitosan is blown assisted by compressed air (to form the droplets) into the alkaline solution. After centrifugation and filtration the particles are washed with hot and cold water. To control the size of granules the pressure of the air and the diameter of the spray-nozzle can be varied (21). To impact the drug release different cross-linking agents for the particles hardening should be used (21).

The ***ionic gelation*** method (Figure 11(b)) is based on the interaction between macromolecules with opposite charge. The chitosan solution under constant stirring is added drop wise to polyanionic solution of Tripolyphosphate (TPP). Due to the complexation interaction of the oppositely charged macromolecules, chitosan undergoes the ionic gelation and precipitates in the form of spherical particles (the range of size is from 500 to 710 μm) (21).

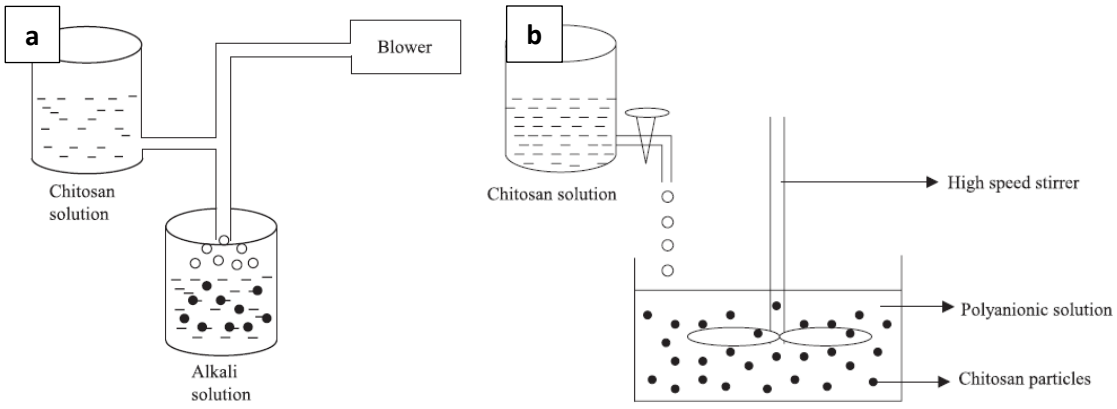

Figure 11 – Layout of coacervation/precipitation method (a) and ionic gelation method (b) techniques (21).

The ***emulsion cross-linking*** method for the preparation of chitosan particulate systems is shown on Figure 12. This technique is based on the fact that chitosan amino groups are able to cross-link with aldehyde groups of the cross-linking agent (21). At first the water-in-oil emulsion of chitosan is prepared. Before being cross-linked with a proper agent, the aqueous droplets in the emulsion should be stabilized by the surfactant. After hardening the granules are filtered, washed and dried. This technique allows producing particles with the size range from 40 to 230 μm. The diameter of the final granules depends from the used cross-linking agent and can be controlled by the speed of stirring and varying the size of aqueous droplets (21).

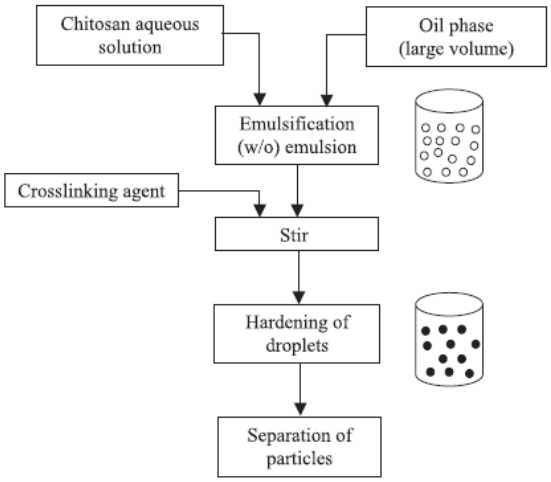

Figure 12 – Schematic representation of emulsion cross-linking method (21).

The ***freeze-drying*** (Figure 13) method allows producing granules by freezing the sprayed suspension and then allows sublimating frozen water due to the pressure reduction. Owing to the sublimation of ice crystals the final granules will have porous structure.

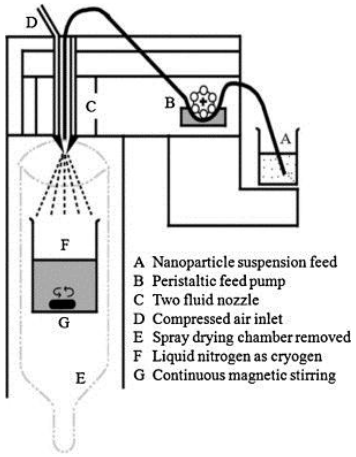

Figure 13 – Layout of freeze-drying technique.

The ***spray drying*** is a well-known and one of the widely-used techniques applied for the production of powders, granules or agglomerates from various mixtures and suspensions. The method is based on the drying of the sprayed suspension under a flow of hot air. The layout of the basic components used in the process of spray drying is represented on Figure 14. The advantage of this technique is that consistent sized particles can be produced from slurry or suspension by rapid drying. To regulate the size and the shape of the final product it is possible to use different kinds of spray nozzle, to vary temperature, the atomization pressure, the spray flow rate and the concentration of the components.

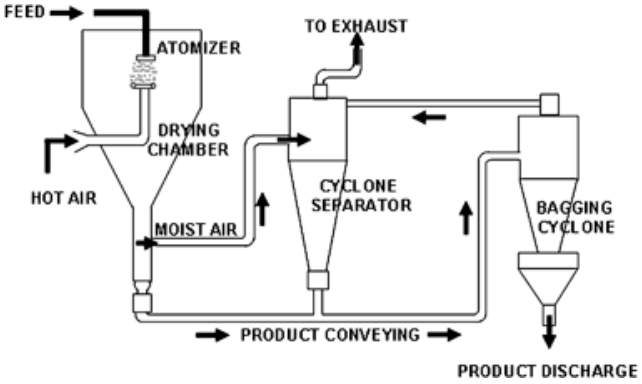

Figure 14 - Layout of spray drying technique.

Spray drying technique allows producing final particles with different morphology (powder, granules, capsules) depending on the composition of initial solution (Figure 15).

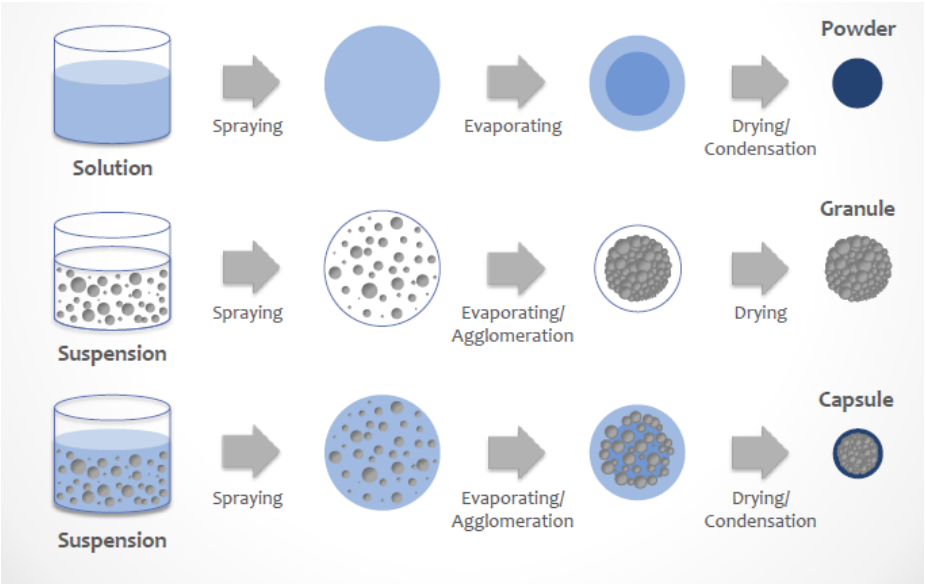

Figure 15 – Schematically illustration of the final particle shape dependence from the initial suspension for spray drying (44).

Spray drying also allows using different type of nozzles with different diameters. In the Figure 16 is schematically presented granules produced by 2-fluid and 3-fluid nozzle.

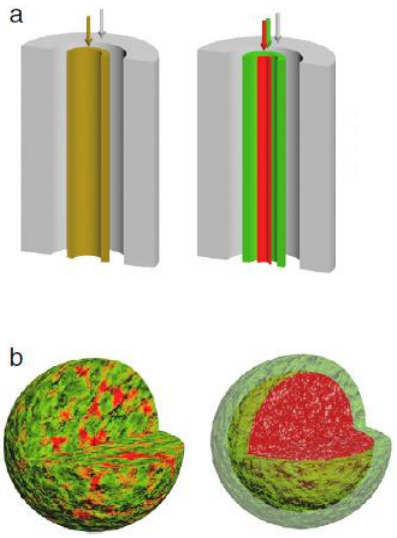

Figure 16 – (a) Scheme of a 2-fluid and a 3-fluid nozzle (cross-section). (b) Schematic droplet structures produced by 2-fluid (left) and 3-fluid (right) nozzles **(85)**.

Some of the techniques applied for the synthesis of chitosan particles (coacervation/precipitation, ionic gelation, emulsion cross-linking methods) can be used for the production of composite granules, if hydroxyapatite is added to the initial components. However, spray drying and freeze-drying methods are preferable.

2.3.3. Chitosan-based DDS.

As it was already mentioned above CH is widely used in different fields of medicine and dentistry in different forms (Figure 17). Chitosan-based DDSs found the wide application for dental, buccal, gastrointenstinal, colon and gene delivery. Due to its muco/bioadhesive properties CH is an outstanding polymer for buccal delivery in form of tablets and films. The solution of CH can also be used for the buccal delivery of proteins, however to obtain prolonged release it is preferable to use CH in form of films or hydrogels. CH can be used as an effective material in different fields of dentistry, for example, in endodontics, CH can be used as dressing anti-inflammatory material for root canal. It was shown that CH stimulates fibroblastic cells, which decreases time of wound healing (45).

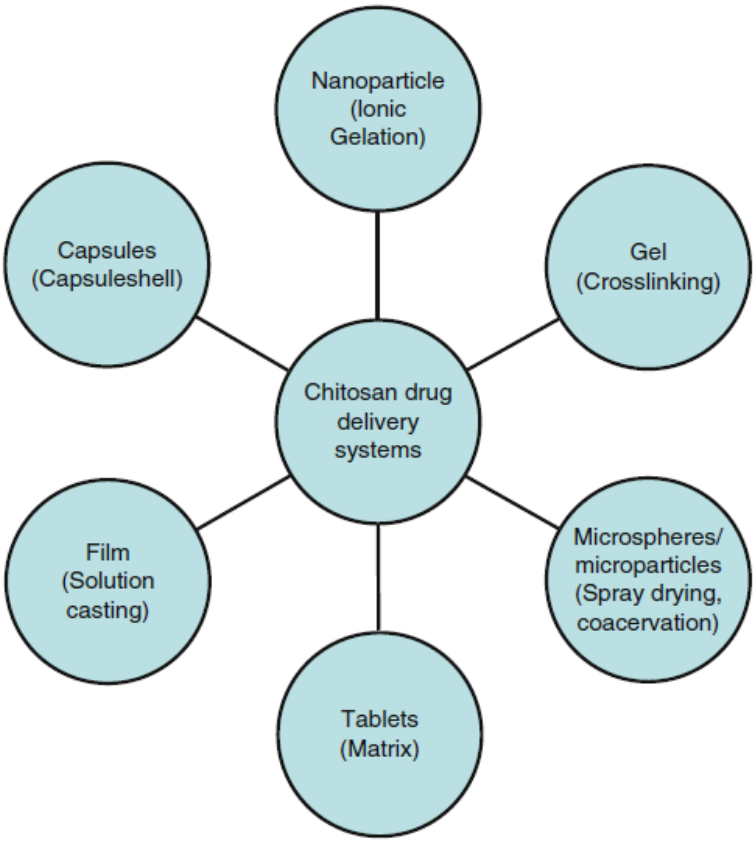

Figure 17 – Different types of chitosan-based DDS (45).

CH combines both bioadhesion and floating abillities that makes CH very promising material for gastroretentive DDSs. Chitosan-based delivery systems can provide ideal characteristics for slow drug release in the stomach (45).

Recently it was founded that CH enhances the drug absorption trough mucosae without damaging the biological system during mucosal drug administration (ocular, nasal, buccal, gastro-enteric and vaginal-uterine therapy). It was shown that CH microparticles are very promising for vaccine delivery systems (21).

There are works aimed to use CH-based DDSs for cancer therapy. Gadolinium neutron capture therapy is one of the novel types of cancer therapy. It is based on injection specific Gd-contained compound into the area with tumour and following irradiation with thermal neutrons. This allows to achieve a high temperature inside cancer cells and destroy them. Gadopentetic acid-loaded CH nanoparticles were used as DDS for cancer therapy by this method (21).

Due to its biodegradable and biocompatible characteristics, together with the ability to form a complexes with DNA through electrostatic interactions CH is one of the most prominent material for gene delivery. Nowadays gene delivery allows treatment of genetic disorders, which were incurable some decades ago (21,45).

2.4. Dexamethasone (DEX)

2.4.1. DEX properties

Dexamethasone (DEX) is a synthetic glucocorticoid class of steroid drugs which chemical structure is illustrated in Figure 18 and summary of characteristics are presented in Table 3. It is frequently used as an anti-inflammatory drug. DEX is a synthetic version of a natural hormone produced by the adrenal glands. Since it is glucocorticosteroid, DEX has a wide range of actions on many parts of the body (46). Recent studies have demonstrated that DEX overcomes inflammatory effects (39) the *in vitro* use of dexamethasone promotes the formation of mineralized nodule of osteoblasts. DEX can also stimulate the proliferation of osteoprogenitor cells and their differentiation into osteoblasts (47).

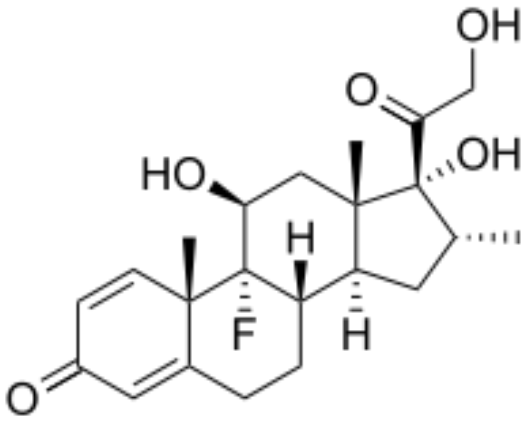

Figure 18 – Chemical Structure of Dexamethasone **(50)**.

The main effects of dexamethasone are due to its anti-inflammatory properties and its ability to alter immune system responses. “Dexamethasone decreases inflammation by suppression of neutrophil migration, decreased production of inflammatory mediators and reversal of increased capillary permeability; suppresses normal immune response. Dexamethasone's mechanism of antiemetic activity is unknown” (48). It is also used in the treatment of certain blood cancers (such as leukemias) by making some cancerous white blood cells undergo self-destruction (46).

Table 3 – Summary of DEX characteristics. (49-50)

Molecular Formula	$C_{22}H_{29}FO_5$
Molecular Weight	392.46
Colour	white to pale yellow
Melting Point	255-261 °C
Solubility in water (25 °C)	0.1mg/ml
Solubility in ethanol, DMSO, DMF	25 mg/ml
Biological half-life	36-54 hours
Duration of metabolic effect	72 hours

Dexamethasone is used in the treatment of various diseases (51):

- Inflammatory disorders (rheumatoid arthritis)
- As a part of cancer treatment therapy:
    - *As a drug treatment:* For example may help reduce swelling in the brain (caused by a brain tumour), spinal cord or bones. Used for leukaemia's and lymphomas treatment along with chemotherapy
    - *To manage sides effect of the therapy*. Nausea treating associated with chemotherapy; as palliation in leukaemia or lymphoma.
- Addison's disease (chronic endocrine system disorder of non-producing sufficient steroid hormones by the adrenal glands);
- To prevent transplant rejection;
- Alergic disorders (asthma);

The side effects strongly depend from the treatment duration and used drug dosage. It is possible following common sides effects: increased appetite; trouble sleeping; excess fluid or swelling in the face, hands, or feet; weight gain; slowed wound healing; increased blood glucose levels. Less common side effects: headache; feeling dizzy; mood swings; low blood potassium level; muscle weakness; high blood pressure; feeling restless; skin rash; menstrual changes; bone or muscle pain and others. Among rare side effect the next could be diagnosed (probability is higher for lon-term use): bleeding or ulcers in the digestive tract; vision changes; change in heart rhythm; congestive heart failure; allergic reaction, with symptoms like trouble breathing or swelling of the face, lips, tongue, or throat after injections of the drug; etc. (46,48, 50)

2.4.2. Drug Delivery Systems of DEX

Nikolas J.S. London *et al* reported that DDS with DEX is one of the most recent additions to the macular edema treatment. Dexamethasone drug delivery systems with commercial name The Ozurdex® was approved by the United States Food and Drug Administration (FDA) for the treatment of macular edema. The Ozurdex® is biodegradable intravitreal implant loaded with 700 µg of DEX (52).

Jun Sik Son *et al* studied (53) HAP scaffolds with the surface containing Dex-loaded PLGA microspheres (Figure 19). It was shown that the release after 2days of the non-immobilized microspheres had an early burst of approximately 35% of the total DEX. The initial burst release was followed by a sustained release of the rest of the drug over the next 30 days. The profile of the drug release from microspheres immobilized on HAp scaffold surface was similar to profile of non-immobilized microspheres, just with lower amount of the released DEX. It was reported that kinetics of both drug releases followed an almost zero-order release. The first order release kinetic was explained due gradual depletion of DEX in the polymer. They have also concluded that DEX release took place by controlled molecular diffusion of DEX through the PLGA polymer either dissolution controlled or an erosion controlled mechanism (53).

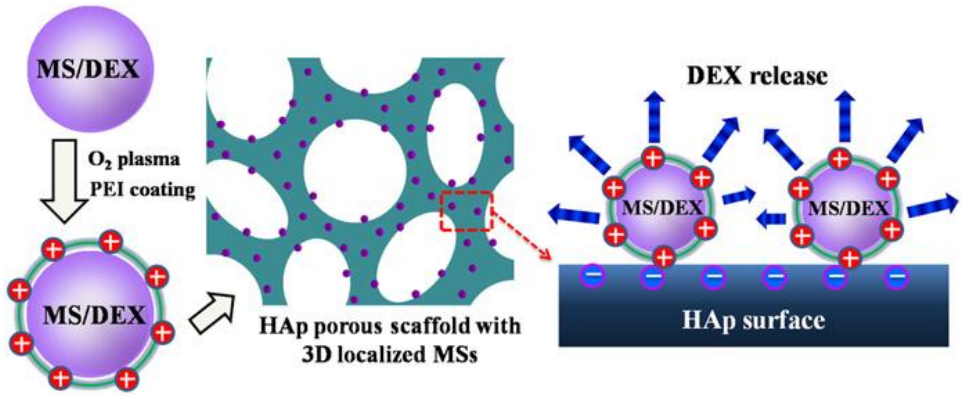

Figure 19 – HAP scaffold containing DEX-loaded PLGA microspheres (53).

Chapter 3

Problem Formulation

3. Problem Formulation

This research studies the drug release process from composite (HAP/CH) nanostructured granules. Granules loaded with DEX were prepared by spray drying technique. The effect of HAP/CH ratio on granules microstructure and drug release behaviour were analysed and investigated.

In order to obtain a core-shell structure the granules were produced by two stage spray drying. First, granules from pure HAP loaded with DEX were spray dried. Afterwards, the granules were immersed into the solution of CH in acetic acid and the final suspension was spray dried.

To reduce swelling of CH the cross-linking agent (GA) was used. The change of drug release behaviour was compared of non- and cross-linked DDS.

The obtained results were compared with different mathematical models of drug release and the most adequate model was fitted for the DDS under study.

Chapter 4

Experimental Procedure

4. Experimental Procedure

The experimental part of the research is divided into four sections: spray drying of granules with different (HAP/CH) ratio and loaded with Dexamethasone; double spray drying of non- and cross-linked granules; drug release from the produced granules; modelling of the drug release profile.

The overall scheme of the experimental procedure is described in Figure 20.

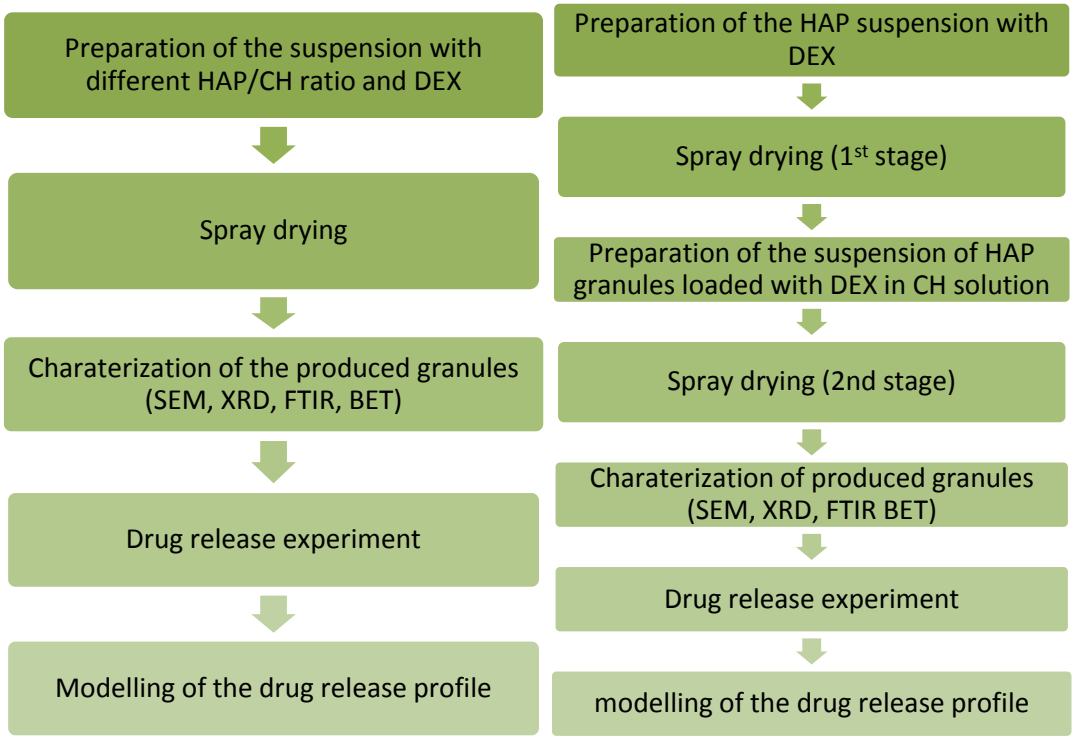

Figure 20 – Scheme of the experimental procedure.

4.1. Materials

The materials used for spray driying were as follows: (1) Comercial ***suspension*** of **Hydroxyapatite** nanoparticles (5 wt% HAP nanoparticles, nanoXIM) from Fluidinova,; (2) ***Chitosan*** with a deacetylation degree ≥ 75% from Sigma-Aldrich, Iceland; (3) ***Dexamethasone*** (96% purity) from ACROS organics, USA; (4) ***Ammonia solution*** (98% purity)from Sigma-Aldrich, Germany; (5) ***Acetic acid solution*** (96% purity), from Sigma-Aldrich, Germany; (6) ***Glutaraldehyde*** (25% in H_2O) from Sigma-Aldrich; (7) phosphate

buffer solution (***PBS)*** 0,01M from Sigma-Aldrich; (8) ***Dialysis membranes,*** 12-14000 Daltons from Medicell International Lt.

4.2. Preparation methods

4.2.1. Preparation of granules by single spray drying

Suspensions with different HAP/CH ratio (Table 4) were prepared as follows: firstly, under constant stirring, chitosan was dissolved in the 2M solution of acetic acid. Then, HAP suspension (0,1 wt %; nanoXIM) with a pH stabilized at 6,5 with ammonia was added to the CH solution. Finally DEX was added to the resulting suspension which was stirred and sonicated for 30 min until complete drug dissolution (0,1 mg/ml). The final suspension was spray dried using a laboratory spray dryer (Mini Spray Dryer Buchi-191, Figure 21(a)). The operational parameters of spray drying are presented in Table 5.

Table 4 – Materials and reagents used for the production of composite granules.

	Composition	**Materials and reagents* for 310 ml of suspension**			
		CH	**HAP (5% wt suspension)**	**DEX**	**GA (1% wt solution)**
Spray drying	***CH+DEX***	0,625 g	-	0,031 g	-
	HAP:CH [1:2]+DEX	0,625 g	6,25 ml	0,031 g	-
	HAP:CH [1:2]+DEX+GA	0,625 g	6,25 ml	0,031 g	0,125 ml
	HAP:CH [2:1]+DEX	0,156 g	6,25 ml	0,031 g	-
	HAP+DEX	-	6,25 ml	0,031 g	-
Double spray drying	***HAP:CH [1:2]+DEX***	0,6250 g	6,25 ml	0,031 g	-

* - The solution of acetic acid was used to dissolve CH and the ammonia solution was used to regulate the pH of the suspensions

4.2.2. Preparation of granules by double spray drying

For double spray drying the granules were prepared in 2 stages:

- The suspension of HAP (0,1 wt %) was stirred and sonicated with DEX (10 wt % with respect to HAP) for 30 min until complete drug dissolution. The resulting suspension was spray dried using the same functional parameters as mentioned in Table 5 and granules were collected.
- The collected spray dried granules were then added to a solution of CH in acetic acid having a pH of 6,5. The quantities of granules and CH were adjusted

according to the desired (HAP/CH) ratios. The final suspension was stirred and then spray dried (Table 5).

4.2.3. Preparation of cross linked granules

To cross link the polymer a solution of glutaraldehyde was added to the HAP/CH suspension (0,2 wt % of glutaraldehyde with respect to CH) before the spray drying step.

4.2.4. Spray drying step

Spray drying is a well-known and widely-used technique for the production of powders, granules or agglomerates from various mixtures and suspensions. The method is based on the drying of a sprayed suspension under a flow of hot air. Spray dryer used in the present work and the layout of the basic components used in the process of spray drying are presented in Figure 21(a-b).

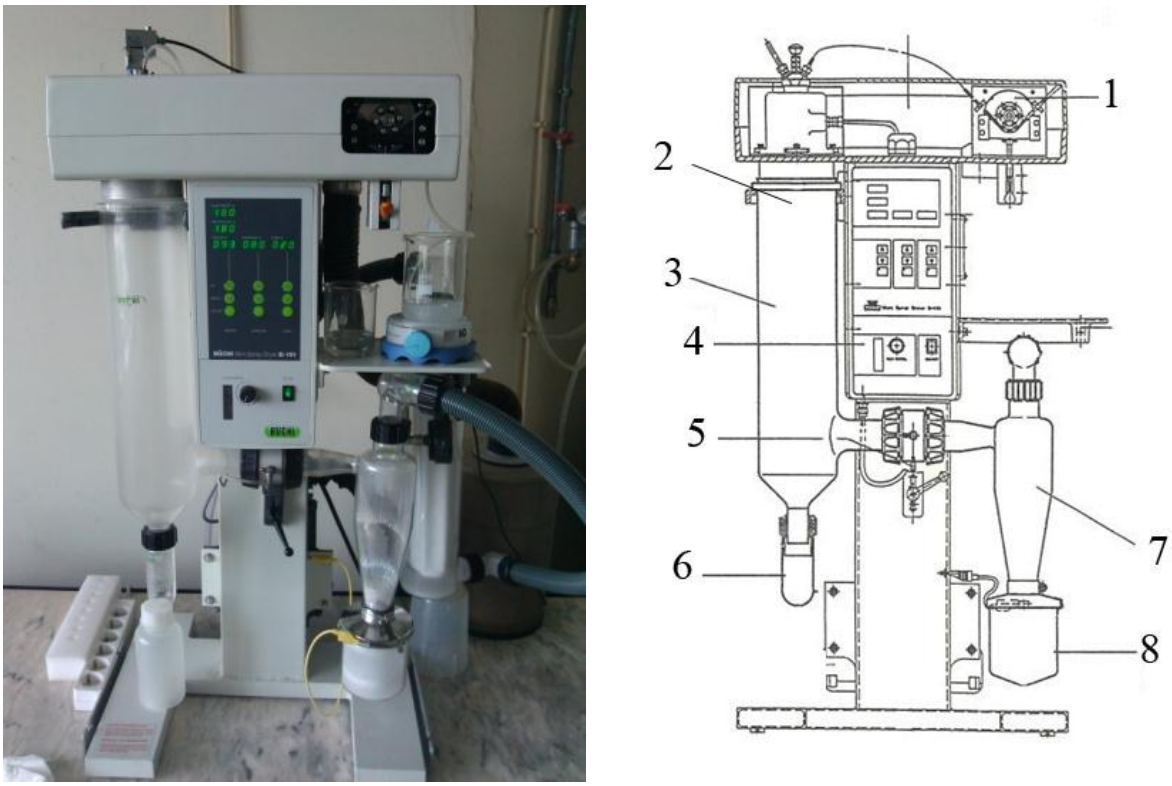

Figure 21 – (a) Mini Spray Dryer Buchi – 191; (b) – Schematic layout of the spray dryer (54): 1 – feeding pump; 2 – nozzle; 3 – atomization chamber; 4 – aspiration regulator; 5 – outlet temperature sensor; 6 – container for big particles; 7 – cyclone; 8 – container for spray dried granules.

The advantage of this technique is that regularly sized particles or granules can be produced from slurries or suspensions by quick drying. The control of the size and shape

of the final particles or granules can be achieved by using different kinds of spray nozzles, by varying the temperature, the atomization pressure, the feeding rate and the concentration of the solution or suspension components.

Table 5 – Operational parameters of spray drying

Pumping	20%
Aspiration	80%
Spray drying temperature	180 °C
Air flow velocity	500 l / h
Nozzle type	2 fluid nozzle

4.3. Materials characterization

The characterization of the spray dried (HAP/CH) granules was carried out by the following methods: X-Ray diffraction (XRD), Scanning Electron Microscopy (SEM), N_2 adsorption with BET isotherms, Fourier Transform Infrared Spectroscopy (FTIR). The evaluation of the released DEX was made by Ultraviolet–visible (UV-vis) spectroscopy.

4.3.1. X-Ray Diffraction analysis (XRD)

X-Ray Diffraction analysis (XRD) is one of the diffraction methods used for studying the structure of matter. It is based on the phenomenon of X-ray diffraction by three-dimensional crystal lattice. X-rays are generated in an X-ray tube; afterwards they are collimated and directed to the sample. The intensity of the reflected X-rays is recorded by the detector, which rotates together with the sample holder. The sample rotates at an angle θ, while the detector rotates at an angle of 2θ. According to Bragg's law, after interaction with a sample the X-ray beam will be diffracted at a specific angle correlated to the periodicity and the arrangement of the crystal structure.

XRD analysis (Rigaku PMG-VH) using monochromatic CuKα (1,5418Å) with radiation at 40kV was carried out to identify the crystal composition of the produced granules. The 2θ scan range was in the interval 3-80° with a scanning speed of 3°/min.

4.3.2. Scanning electron microscopy (SEM)

The morphology (shape and size) of the granules was evaluated by scanning electron microscopy (SEM Hitachi S-4100). The samples of powder particles were glued to an sample holder with carbon tape and then coated with a conductive layer of carbon by

sputtering (EMITECH K950X) to be observed in SEM at 20-25 KV, using different magnifications.

In the scanning electron microscopy (SEM) (Figure 22) the focused beam of low-energy electrons is used to raster along the sample surface. The image of the sample is generated by secondary electrons that are emitted from the surface after being excited by the electron beam.

The interaction of a high-energy electron beam with the sample produces various secondary signals, many of which can be used in electron microscopy. Secondary electrons and backscattered electrons are used for sample imaging. Secondary electrons are relevant for analysing morphology and topography of specimens and backscattered electrons are used for contrast. Diffracted backscattered electrons are used for crystal structure determination and crystallographic orientation of the grains, from which the crystal structure consist. Emitted photons are used for elemental analysis.

The layout of SEM basic elements is presented in Figure 22. On the top of the microscope there is an electron gun that produces the electron beam. The beam is focused by condenser lenses to a spot with a diameter of 0,5 to 5 nm. Before scanning the sample surface the beam passes through pairs of scanning coils of deflector plates in the electron column (where the beam is deflected either linearly or in a raster fashion).

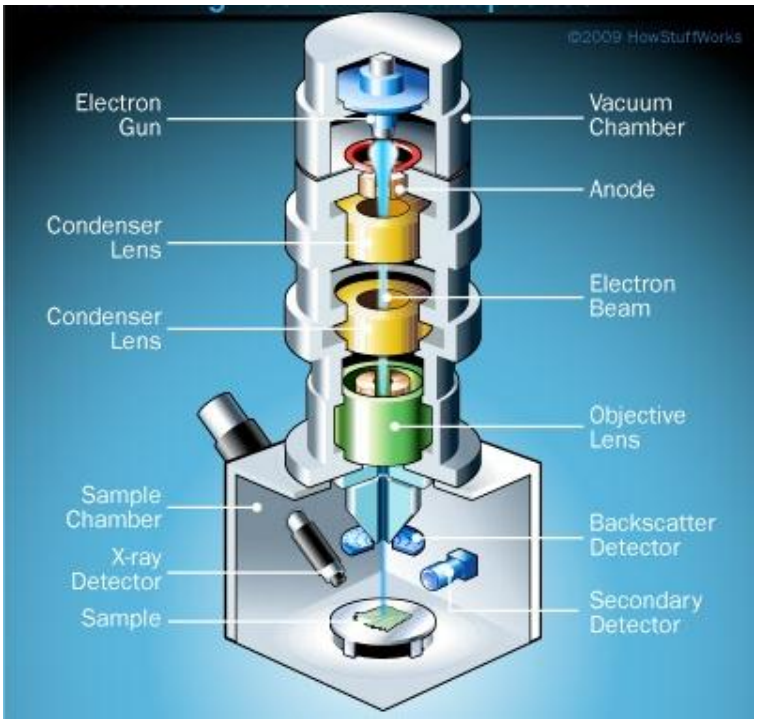

Figure 22 – Schematic layout of SEM (55).

SEM has a significant impact on different science fields: material science, medical science, biology, etc. The scanning electron microscopy provides information about microstructure (materials morphology, i.e. materials shape and size), composition and other properties of a sample with high resolution (55).

4.3.3. Fourier Transform Infrared Spectroscopy (FTIR)

The Fourier Transform Infrared Spectroscopy (FTIR) allows to detect the presence of chemical bonds that absorb incident infrared light of a specific frequency, i.e. chemical bonds which vibrational frequency is the same as the frequency of the incident radiation.

The basic units of a FTIR spectrometer are shown in the Figure 23. The source generates the radiation, which then reaches the sample after being interfered on the interferometer. The detector records the interferogram of the beam passed through the sample. Then, having being intensified by the amplifier, the signal is converted to digital form. Finally, special computer software makes a Fourier transformation and presents the result of the analysis. Modern FTIR systems use the fast Fourier-transformation (FFT) algorithm, which performs faster analysis (56).

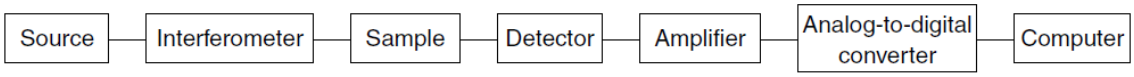

Figure 23 – Basic units of FTIR spectrometer (56).

The function of any kind of interferometer is based on the phenomenon of interference. Basically, the light beam spatially splits into two or more coherent beams. Each of the beams passes the different optical path and returns to the screen, creating an interference pattern. According to this pattern the phase displacement of the beams can be set. The most common interferometer used in FTIR is the interferometer designed by Albert Abraham Michelson (Figure 24).

The principle of ***Michelson interferometer*** work can be described by the following steps:

1. The light coming from the light source is divided by a semi-transparent beam splitter into two coherent beams.
2. One beam is directed to a stationary mirror and reflected back from it on the beam splitter.

3. The other beam goes to a moving mirror and then it is also reflected back to the beam splitter. On the beam splitter both beams are recombined.
4. These two coherent beams interfere with each other, due to the changes in the relative position of the moving mirror to the fixed mirror. Depending on the difference in the path between beams, they can either enhance or weaken each other. In the focal plane of the lens interference bands can be observed and recorded by the detector.
5. Detector registers the intensity of the interferogram, which contains complete information about the spectral composition of the radiation coming from the source and passing through the sample.

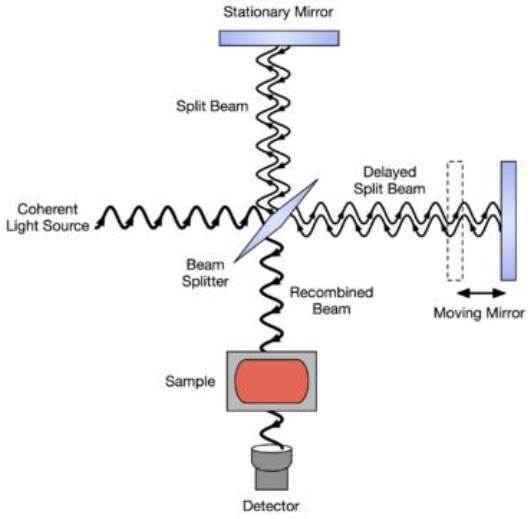

Figure 24 – Layout of the Michelson interferometer used for FTIR (57).

If the sample absorbs the radiation with a certain frequency, the intensity of the interferogram will be decreased correspondingly to this frequency. After the Fourier transformation made on the computer, the resulting spectrum will show the absorption band of the sample.

FTIR spectroscopy has some distinct advantages in comparison with other spectrometer techniques:

- High resolving power and fast scanning.
- Constant resolution over the whole spectral region.
- High accuracy of the determination of the number of waves.
- Possibility to study a wide spectral range during a single scanning.
- Possibility to detect a weak signal.
- Simple design with only one moving part (moving mirror).

Powerful computers and software perform a wide possibility of processing with data apart from Fourier transform (baseline correction, smoothing, integration, library searching, etc.) (56,58-59).

The samples were powdered, mixed with KBr, and pressed as pellets. FTIR spectra were recorded at 48 scans with a resolution of 2 cm^{-1} (FTIR Mattson 7000).

4.3.4. Gas adsorption: BET analysis.

Solids can adsorb the condensable gases. The value of the adsorbed gas depends on the material of the solid and the nature of the gas. Significant influence in the adsorption phenomena that occurs on the solids is made by two factors: the surface area of a solid and its porosity. Thus, measuring the gas adsorption allows getting information about the specific surface area and pore structure of a sample.

The BET analysis provides precise evaluation of a specific surface. The BET theory explains the adsorption of gas molecules on a sample surface. It was developed by Stephen Brunauer, Paul Emmett and Edward Teller in 1938.

Being placed into the closed space filled with gas at certain pressure, sample starts to adsorb the gas. The mass of the sample increase and the pressure of the gas decreases. Later the pressure becomes constant and the sample mass stops increase. If the volume of the sample and the space, where it was placed, are known based on the pressure reduction and using ideal gas law the amount of the adsorbed gas can be calculated. The amount of the adsorbed gas will be proportional to the sample mass, the nature and the pressure of the gas and temperature (60-61).

The measured volume of used gas at different pressure allows building adsorption isotherms. The shape of the isotherm describes the interaction between gas and sample. Depending on the type of the isotherm it is possible to make conclusion about the surface area and the porosity of the material. Figure 25 shows five possible types of isotherms. Type I isotherm is often called “pseudo-Langmuir isotherm” it is attributed mainly to microporous samples with relatively small surface. Type II is the most common isotherm obtaining during BET analysis. It is typical for non-porous or macroporous materials. The start point of the straight middle part of the isotherm is used for the relative pressure at which the monolayer adsorption is completed determination. Type III is relatively rare type of isotherms. It can be used for BET, since there is no asymptote in the curve, what means that monolayer was not formed. Type IV is associated with capillary condensation

in the pores, which is characterized by a larger slope at higher relative pressure. The initial part of the isotherm is similar to the type II and showed the formation of monolayer with following formation of multilayers. This type of isotherms is attributed to mesopores materials. Type V is a variety of type III isotherm when there are mesopores in sample. This type of isotherm is not applicable for BET analysis (60-61).

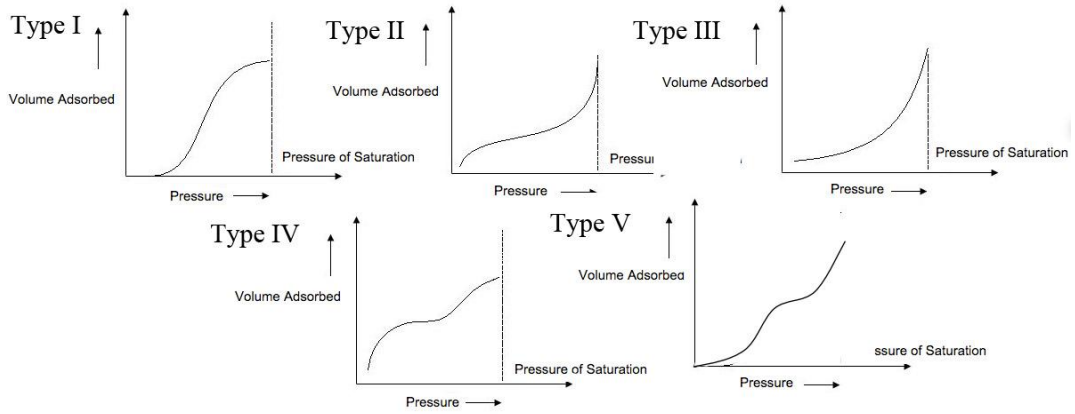

Figure 25 – Types of isothermes (60).

Porous materials can be classified by the shape and size of pores. The IUPAC classification of pore size is following: micropores are pores with the size less than 2 nm; mesopores are pores between 2 and 50 nm; pores bigger than 50 nm are called macropores. The determination of pore shape can be done according the shape of hysteresis loop on the isotherm. Figure 26 presents 4 different types of hysteresis loops. (61)

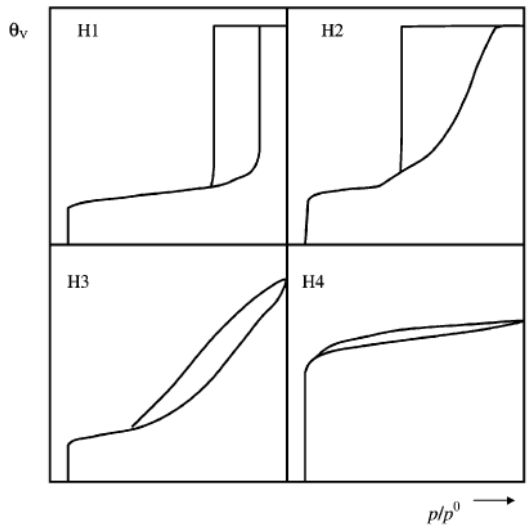

Figure 26 – IUPAC classification of adsorption hysteresis loops (61).

Type H1 is usually attributed to the material with narrow distribution of relatively uniform pores. More complex network pore structures with not well-defined shape show H2 type adsorption hysteresis loop. H3 loop is observed with non-rigid aggregates of plate-like particles with slit-shaped pores. Type H4 is associated with samples containing meso- and micropores (61-62).

BET is based on the kinetic model of adsorption processes, which was purposed by Langmuir. The most common equation describes BET is following:

$$\frac{P}{V_a(P_0 - P)} = \frac{1}{V_m C} + \frac{C - 1}{V_m C}\left(\frac{P}{P_0}\right) \quad (9)$$

Where V_a – volume of adsorbed gas at pressure P; V_m – volume of adsorbed gas when surface is covered with a monolayer; P is saturation pressure; C is BET constant attributable to the energy of absorption in the first adsorbed layer (61-62).

For an accurate measurement sample must be degassed (in vacuum) to remove water and other contaminants. After the sample is degassed it is moved into the analysis port (Figure 27), where it is cooled with liquid nitrogen. To measure gas adsorption low temperature must be maintained; thereby it will be rather strong interaction between gas molecules and sample surface. Afterwards the sample is removed from N_2 atmosphere and heated to release and evaluate the amount of adsorbed gas. Final data is presented in the form of BET isotherms (the amount of adsorbed gas is a function of the relative pressure). The use of the obtained isotherms allows calculating total surface area.

For BET analysis nitrogen is used, due to its strong interaction with a samples surface and its availability. Since helium it is not adsorbed by sample surface it is used for volume calibration of the sample cell (60).

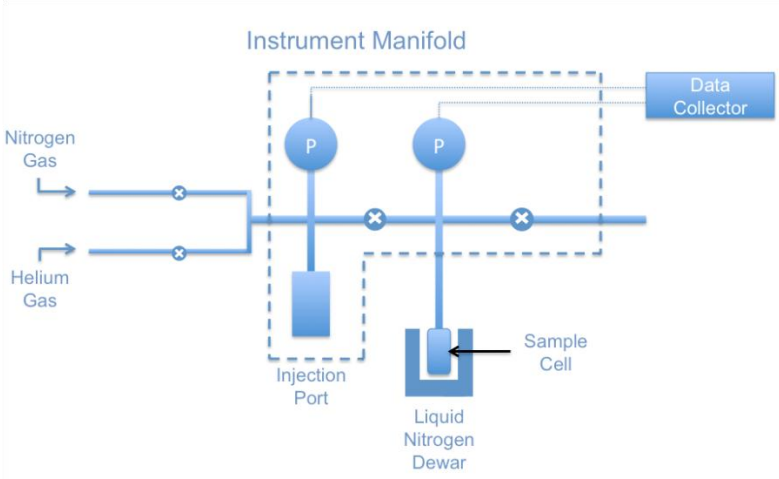

Figure 27 – Schematic layout of the BET instrument (60).

To evaluate the specific surface area and the average pore size the BET (Brunauer, Emmett and Teller) analysis (Micromeritics Gemini 2370 V5) was carried out and the obtained isotherms of adsorption/desorption nitrogen were analysed.

4.3.5. UV-vis spectroscopy.

Different types of molecules absorb a radiation with specific wavelength. UV-vis spectroscopy allows detecting the presence of chemical functional groups with valence electrons. The absorption of visible and ultraviolet (UV) radiations is associated with the excitation of electrons to higher energy states. This excitation of electrons to higher energy state is accompanied by the absorption of some amount of energy from the incident light which leads to decrease in intensity of light being transmitted.

UV-Vis wavelength range generally corresponds to 200 – 1000 nm and therefore partly includes near infra-red (NIR). The limits of the range are determined by detectors and light sources as well as the materials brought into contact with radiation. Figure 28 illustrates the basic structure of spectrophotometer. Electromagnetic radiation in UV-Vis range is generated by an appropriate *light source*. A good light source should produce sufficient energy or power. A *monochromator* disperses the light in order to select a narrow bandwidth as the incident radiation. Light dispersion, however, can be obtained by both gratings and prisms. The sample container, known as a cell or cuvette, is made of a transparent material. Some typical materials used are fused silica, quartz and glass. The sides of these cells should be highly polished to keep reflection and scatter losses to a minimum. *Detectors* collect the light transmitted from the sample and convert it into measurable current. The amount of produced current is proportional to the amount of light reaching the detector. Major detectors used are phototube, PMT, photodiode, photodiode array, CCD array etc.

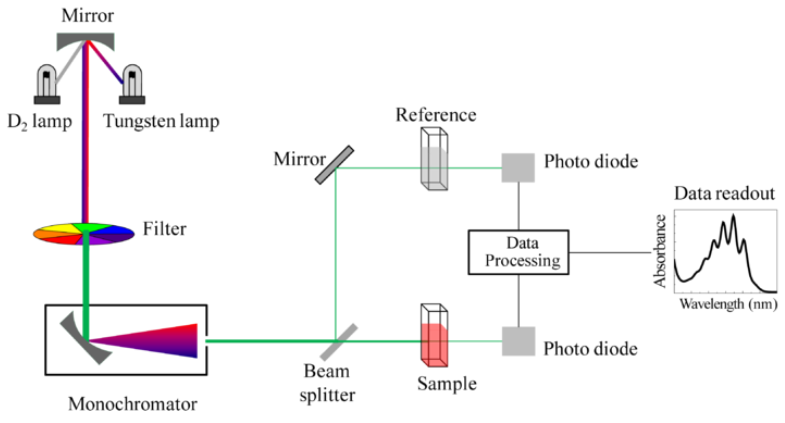

Figure 28 - Schematic layout of the UV- visible spectrophotometer (63).

The quantification of the released drug (dexamethasone, DEX) was made by UV-vis spectroscopy using a Shimadzu UV-3100 spectrophotometer linked to 2:10 UVProbe programme. The DEX concentration in each sample was calculated using a standard calibration curve (the curve was obtained previously with different DEX concentrations in PBS), relating the DEX concentration with the absorbance. A fresh medium of PBS was used as a reference during the analysis (64).

4.4. Drug release experiments

For an *in vitro* drug release experiment, a certain amount of DEX-loaded composite granules was loaded into a dialysis membrane tube and then added with 4 ml of PBS at pH=7.4. Afterwards the membrane was placed inside a conical flask with 200 ml of PBS at pH=7.4 (Figure 29). This system was then placed into the incubator hood (Buhler TH15) (Figure 30) at 37 °C and with a constant stirring (125 min^{-1}). Aliquots of 4 ml of the supernatant liquid were taken periodically at different time intervals. An equal volume (4 ml) of fresh PBS was added to the system every time after every aliquot withdrawal. The amount of the released DEX into the solution was measured by UV spectrometry (Shimadzu UV-3100 PC) at 241,5 nm. The concentration of the drug was calculated using a calibration curve (Appendix).

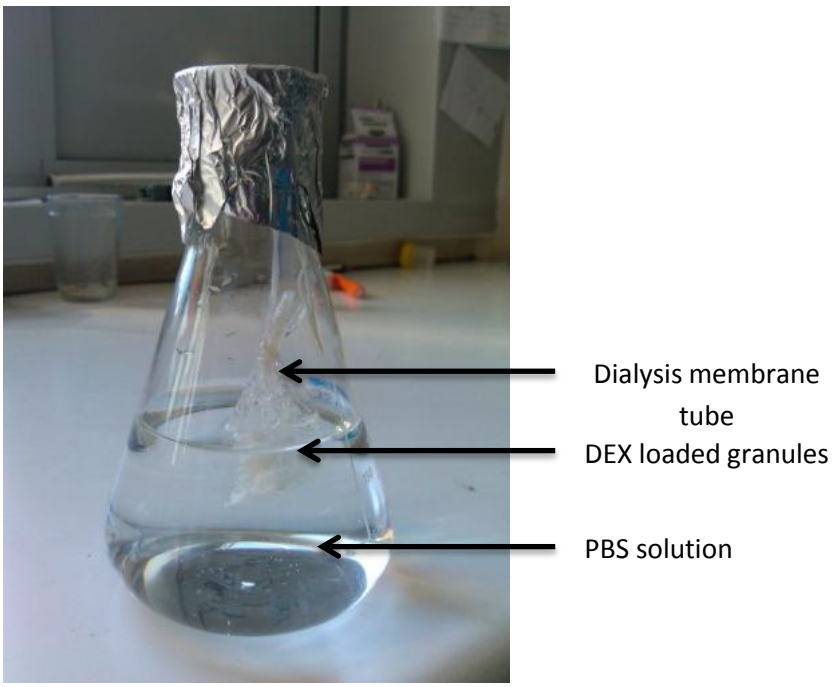

Figure 29 – The scheme of the drug release experiment.

To be used in the in vitro drug release experiment, the dialysis membrane tube requires pretreatment. For its protection the stock membrane is covered with glycerine, which must be removed before the use in the experiment. The cleaning was carried out according to the instruction (65): the membrane was heated at 80 °C for 30 min in the aqueous solution (800 ml) containing 2% sodium bicarbonate and 1 millimolar EDTA.

Figure 30 – Incubator hood (Bühler TH15).

4.5. Analysis of the morphology granules after drug release

To analyse the change in the granules morphology, its degradation and swelling, a small amount of granules (2**–**5 mg) was immersed into different containers with 10 ml of PBS solution and kept at 37 °C. After different time intervals the granules were taken out from PBS solution, dried and analysed by SEM. The obtained SEM micrographs will be presented and discussed in the next chapter.

4.6. Identification of the appropriate mathematical model

According to the literature review the obtained results of drug release were compared with different mathematical models, using “DDSolver”, free software. “DDSolver” is a free Excel add-in software package, developed by Yong Zhang et al. for the analysis of drug dissolution data and fitting it to different models by using a nonlinear optimization method (66) Various mathematical models were chosen to fit the data and the best fit was selected. The conclusion on the mathematical appropriateness was made by comparing $R^2_{adj.}$ (adjustment coefficient).

Chapter 5

Results and Discussions

Results and discussions

5.1 Physical and chemical characteristics of spray dried granules

5.1.1. HAP and composite (HAP: CH) granules loaded with DEX

Figure 31 shows the SEM micrographs of the original commercial nanosized HAP particles (Figure 31(a)) and of the corresponding spray dried granules (Figure 31(b)). As observed spray drying allows to convert the initial HAP nanoparticles, which have an average size of ~ 50nm, into uniform spherical granules with a diameter of few micrometres (Figure 31(b)). Moreover it is also noticed that HAP spray dried microspheres present a somewhat irregular and rough surface.

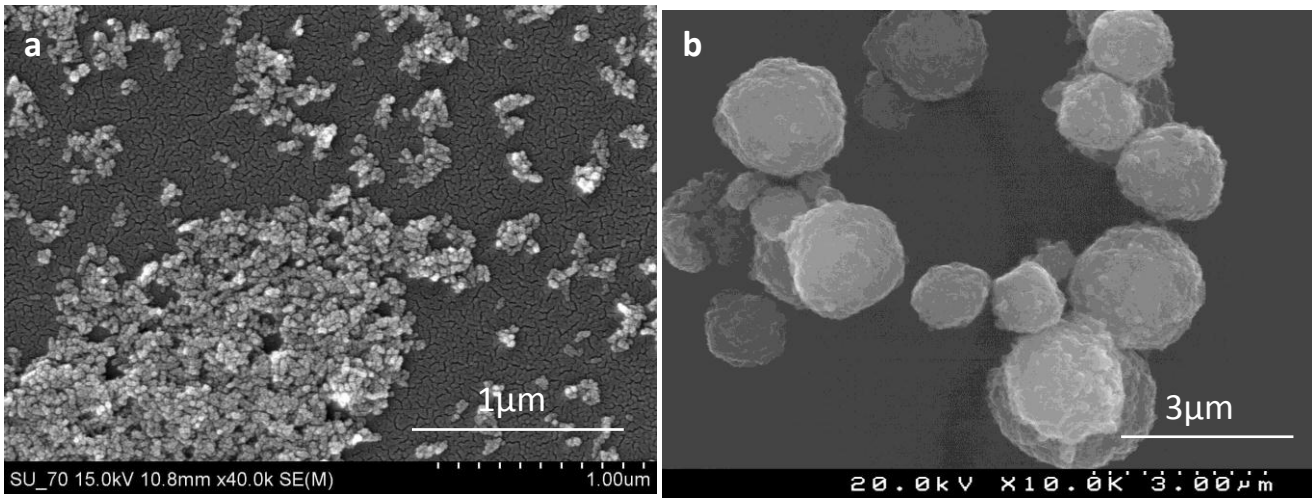

Figure 31 – SEM micrographs of (a) commercial HAP from Fludinova and (b) spray dried HAP granules.

In spite of their compact aspect the spray dried granules have a large specific surface area of 100m^2/g (Table 6) which is comparable to that of the starting nanosized HAP particles (110m^2/g) (Table 6). This indicates that the spray dried granules are porous granules that maintain the nanostructure of the starting HAP nanoparticles.

Regarding the crystallinity of the spray dried granules it was noticed that spray drying did not modify the crystallinity of the initial particles. The X-ray diffractogram of initial HAP nanoparticles is presented in Figure 32. The X-ray diffraction pattern (XRD) of the HAP granules is presented in Figure 35 and it could be confirmed that the XRD of both materials, i.e. initial HAP particles and spray dried particles, were practically undistinguishable.

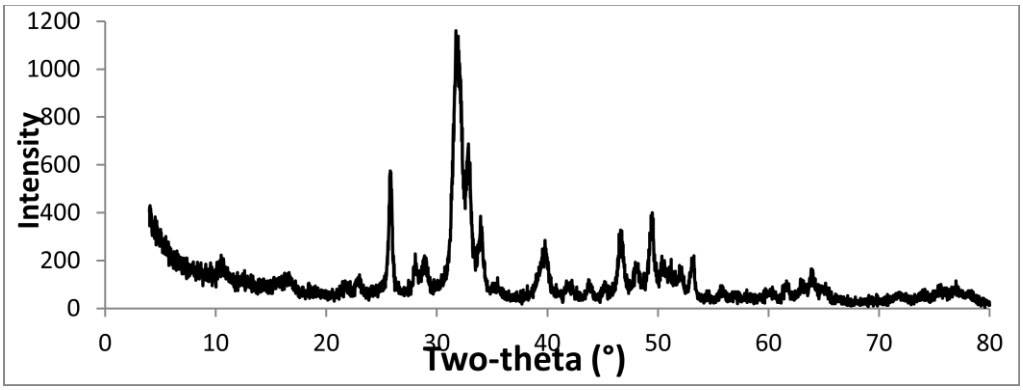

Figure 32 – XRD diffractogram of the starting HAP nanoparticles.

Figure 33 allows comparing the EDS spectra of the initial HAP particles and of the spray dried granules. It is observed that Ca/P ratios corresponding to the initial HAP and spray dried granules are almost the same, i.e. 1,64 and 1,70, respectively, which is very close to the value of standard CA/P ratio in HAP – 1,67 (30). Since spray drying was carried out at 180 °C it is too low temperature to modify HAP. EDS allows to assume that stoichiometry of HAP was not changed

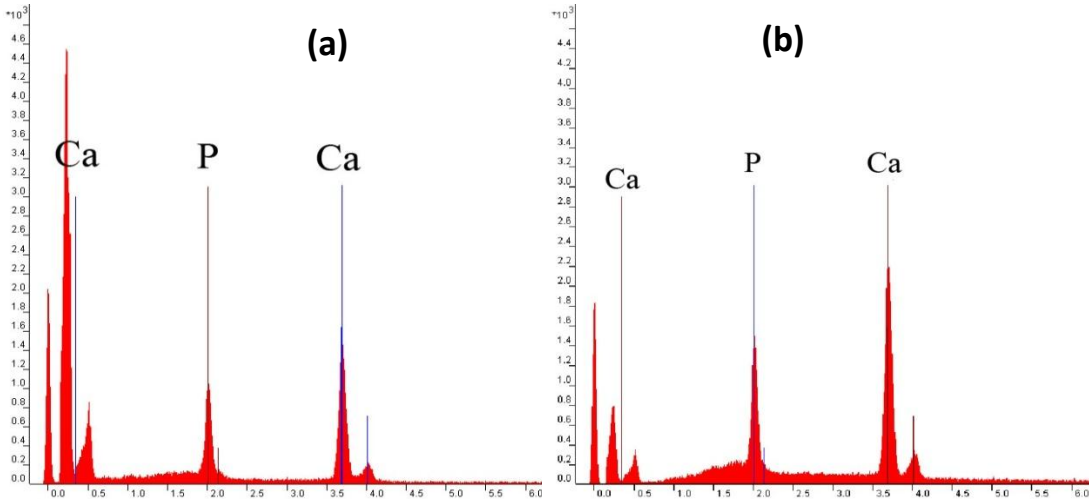

Figure 33 – EDS spectra of: (a) commercial HAP from Fludinova and (b) spray dried HAP granules.

Figure 34 shows the changes of morphology of spray dried granules as DEX and HAP nanoparticles are added chitosan to (CH) solution, for different HAP/CH ratios. Spray dried particles of CH+DEX (Figure 34(a)) can be described as particles of smooth surfaces with some concavities and an average size between 1,5 μm and 3 μm, though larger particles of chitosan 5-6 μm can be also observed. When HAP is also added to

the polymer solution, the spray-dried composite granules, i.e. CH:HAP [2:1]+DEX and CH:HAP [1:2]+DEX, show a tendency to lose their concavities and smooth surface thus acquiring a more spherical shape with a rougher surface as HAP/CH ratio increases. The granules of HAP+DEX composition (Figure 34(d)) have a spherical shape with rough surface and a size of 1-3 μm, being identical to the HAP granules.

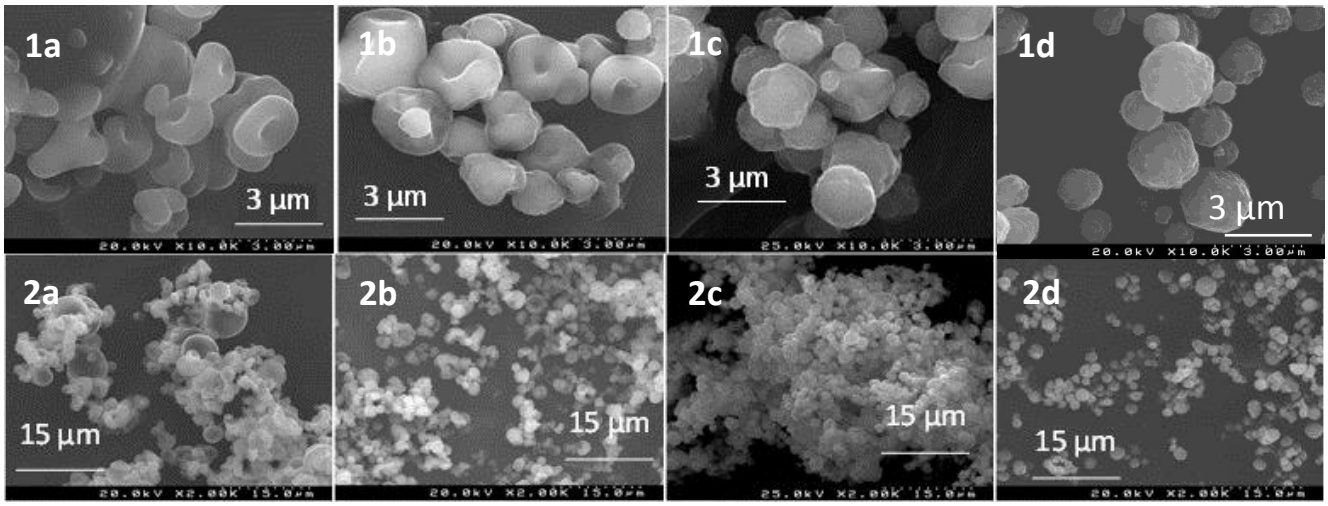

Figure 34 – SEM micrographs with different magnifications of spray dried granules with different HAP/CH ratio: (a) – CH+DEX; (b) – CH:HAP [2:1]+DEX; (c) – CH:HAP [1:2]+DEX; (d) – HAP+DEX

In addition, it was also observed that the measured specific surface area (SSA) of the HAP+DEX granules was 114m^2/g, being this a very close value to that of HAP granules (100m^2/g).

It may be thus concluded that the presence of DEX in the HAP particle suspension did not affect the morphology of HAP granules neither its nanostructured condition. Regarding the composite granules it was observed that their SSA decreases as the CH relative amount in the spray dried granules increases. Table 6 summarizes the SSA of the granules measured by gas adsorption using BET isotherm.

Table 6 – Values of the specific surface area (SSA) of different types of spray dried granules.

Composition of granules	SSA
Initial commercial HAP from Fludinova	110 m²/g
HAP spray dried granules	100 m²/g
HAP+DEX	114 m²/g
HAP : CH (2:1) +DEX	93 m²/g

HAP : CH (1:2) +DEX	10 m²/g
HAP : CH (1:2) +DEX +Glutaraldehyde	52 m²/g
Double spray-drying HAP:CH(1:2)+DEX	19 m²/g

Regarding the crystallinity of spray dried (HAP+DEX) or of the composite (HAP:CH+DEX) granules which XRD patterns are presented in Figure 35, only the peaks corresponding to HAP are observed denoting that spray drying and/or the presence of DEX did not induce the formation of secondary calcium phosphate phases.

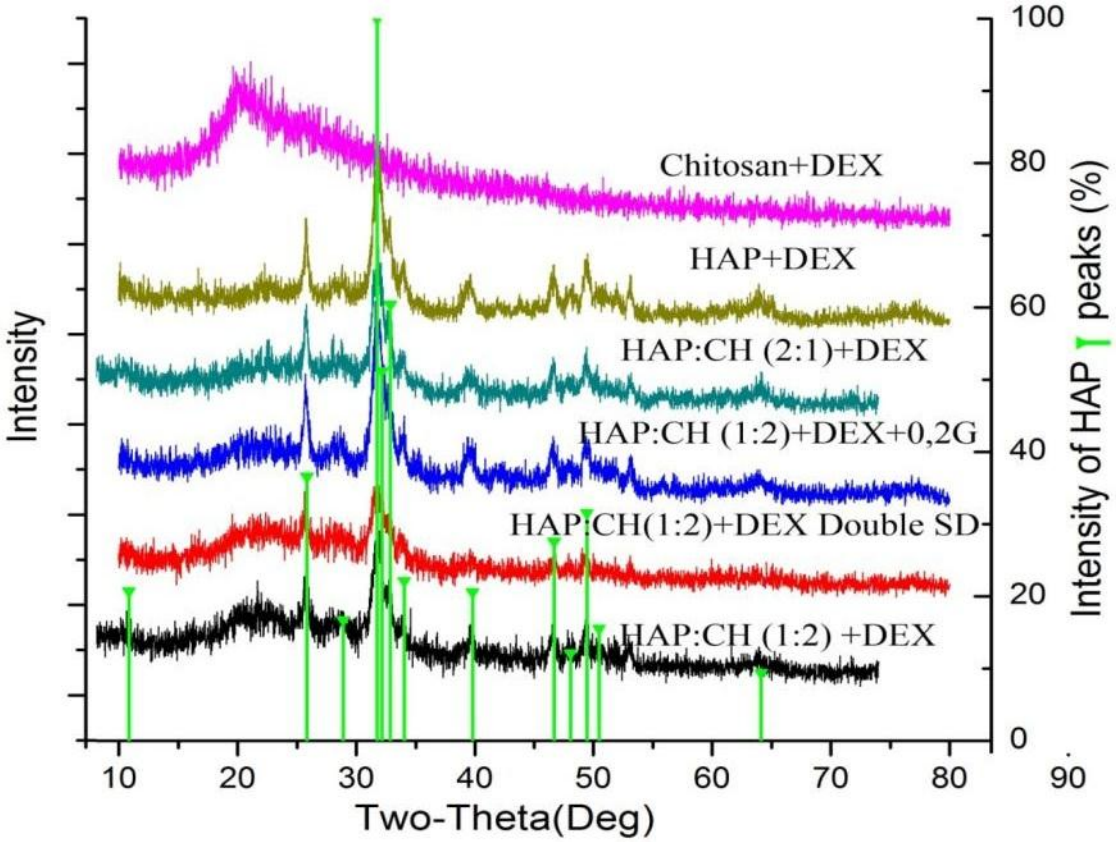

Figure 35 – XRD patterns of different types spray dried granules.

It is also noticed that with the decrease of HAP/CH ratio the HAP peaks become less prominent while the amorphous phase corresponding to CH becomes enhanced. The XRD of CH is shown in Figure 36 for a comparative purpose.

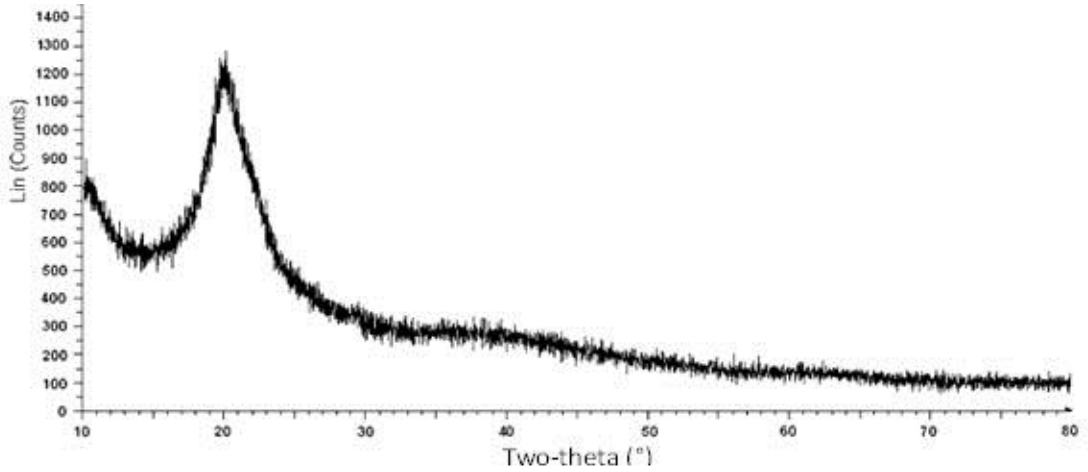

Figure 36 – XRD diffractogram of standard chitosan produced by Sigma Aldrich (67).

Figure 37 shows the Fourier transform infrared (FTIR) spectra of HAP+DEX and of CH+DEX spray dried granules and a standard FTIR of DEX (68).

The FTIR spectrum of HAP+DEX granules shows the characteristic bands of HAP at 473, 558, 600, 1018 cm^{-1} which are attributed to bending vibration of PO_4^{3-} group. Two peaks are also observed at 965 and 1087 cm^{-1} that corresponds to the stretching vibration of phosphate group. A broad peak around 3370 and a small peak 1662 cm^{-1} are in the region where absorbed water is usually observed. A small peak at 3571 cm^{-1} is attributed to stretching vibration of OH^- group.

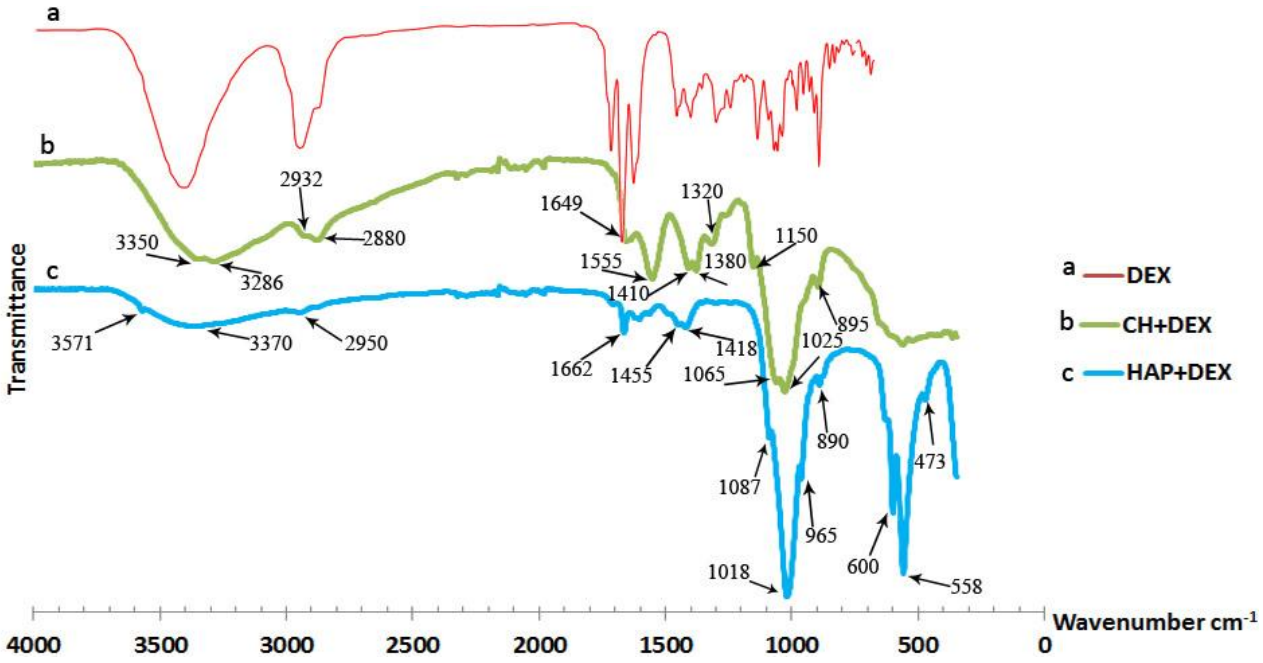

Figure 37 – FTIR spectra of (a) DEX (68), (b) CH+DEX and (c) HAP+DEX spray dried granules.

The spectrum of CH+DEX granules has a well-defined peak at 1025 cm^{-1} due to skeletal vibration of C-O stretching. The bands at around 895 and 1150 cm^{-1} are attributed to glycosidic bondings. The peak at 1320 cm^{-1} is characteristic of C-O-N stretching. The bands at 1380, 1410 and 2880 cm^{-1} indicate the presence of $-CH_3$, $-CH_2$, and –CH groups respectively. N-H bending from amine and amide is indicated by the bands at 1555 and 1649 cm^{-1}. The wave numbers of the peaks referred in the present work, the literature references and chemical bond peaks assignment are presented in the Table 7 (69-72).

Due to overlapping of the main DEX peaks with some characteristic peaks of CH and HAP in the region of 1000-1100, 1500-1700 and 2900-3000 cm^{-1} it is difficult to detect DEX in the spectra of HAP+DEX and CH+DEX. However, it is possible to observe that the characteristic peaks in the regions of 1000 -1100 and 1500-1700 cm^{-1} are more intense for HAP+DEX and CH+DEX granules than for pure HAP and CH mentioned in literature (69).

According to literature (73) the interaction between CH and DEX may be detected by the shift of characteristic peaks of CH (3250 cm^{-1}) and DEX (3390 cm^{-1}) to the wave numbers at 3286 and 3383 cm^{-1}. In the present work the FTIR spectrum of CH+DEX presents a peak at 3286 and it is also possible to observe that the DEX peak lying at 3390-3400cm^{-1} is shifted to 3350 cm^{-1} in the CH+DEX spectrum. This indicates that an effective interaction between the drug (DEX) and CH takes place. The spectra of the composite granules having different HAP/CH ratios are shown in Figure 38. In the same figure are also presented the spectra corresponding the granules cross-linked with glutaraldeide (GA) and to the double spray dried granules. It is generally observed that the FTIR profiles are similar in terms of the shape and intensity of its peaks. Comparing these spectra to those corresponding to (HAP+DEX) and to (CH+DEX), the bands around 1020, 1320-1410, 1555 cm^{-1} are wider and more intensive due to the overlapping of some characteristic peaks of both CH and HAP.

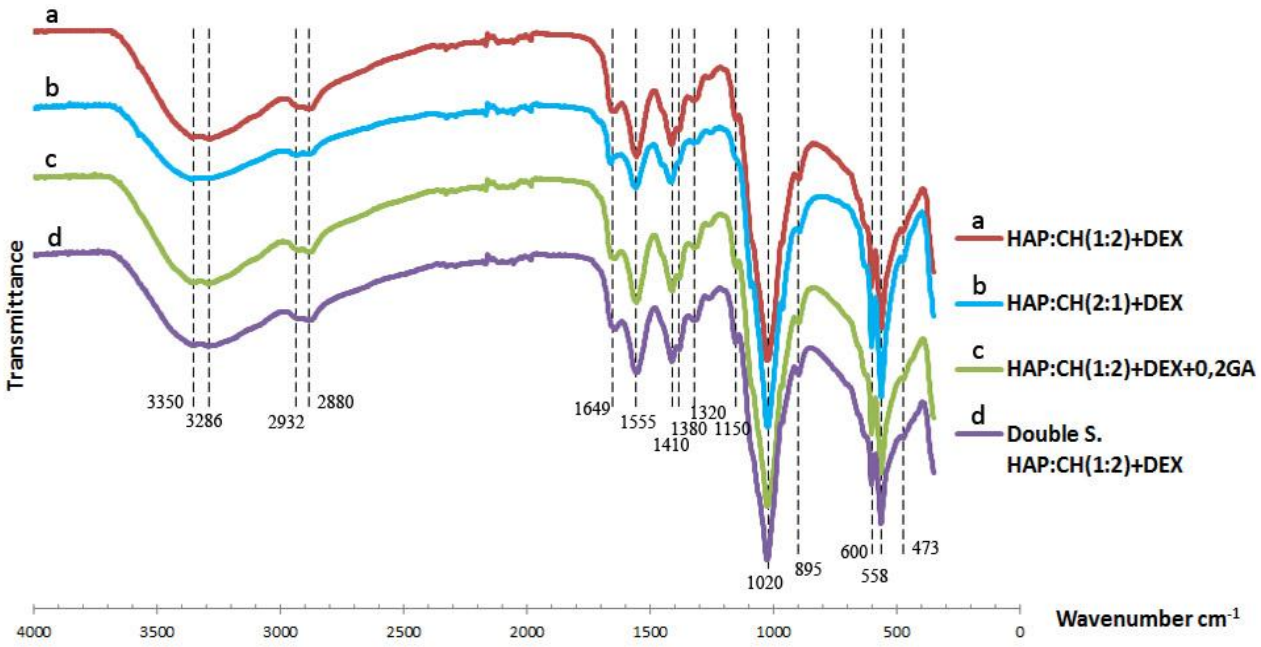

Figure 38 – FTIR spectra of spray dried granules with different (HAP/CH) ratio ((a) and (b)), cross-linked with GA (c) and double spray dried (d).

Table 7 – Summary of FTIR analyses with peak interpretation.

Wavenumber (cm^{-1})		HAP+DEX	CH+DEX	HAP:CH [1:2]+DEX	HAP:CH [2:1]+DEX	HAP:CH [1:2]+DEX +0,2 GA	HAP:CH [1:2]+DEX Double SD	**Chemical bond description**
Reference (70-73)	**Present work**							
470-472	~473	+	-	+	+	+	+	PO_4^{3-} bending vibration(HAP)
565-568	~558	+	-	+	+	+	+	PO_4^{3-} bending vibration(HAP)
602	~600	+	-	+	+	+	+	PO_4^{3-} bending vibration(HAP)
897	~895	+	+	+	+	+	+	glycosidic bonding
962-964	~965	+	-	+	+	+	+	PO_4^{3-} stretching vibration
1026	~1025	-	+	+	+	+	+	skeletal vibration of C-O stretching (CH)
1036-1041	~1018	+	-					PO_4^{3-} bending vibration(HAP)
1070	~1065	-	+	-	-	-	-	C-O-C stretching (CH)
1093	~1087	+	-	-	-	-	-	PO_4^{3-} stretching vibration (HAP)
1150-1154	~1150	-	+	+	+	+	+	antisymmetric stretching C-O-C and C-N stretching (CH) (glycosidic bonding)
1320	~1320	-	+	+	+	+	+	C-O-N stretching (CH)
1375	~1380	-	+	+	+	+	+	CH_3 symmetrical deformation (CH)
1414	~1410	-	+	+	+	+	+	$-CH_2$ bending vibration (CH)
1584-1560	~1555	-	+	+	+	+	+	N-H bending from amine and amide II (CH)
1645	~1649	-	+	+	+	+	+	amide I (CH)
1660	~1662	+	-					absorbed water (HAP)

2864-2878	~2880	-	+	+	+	+	+	C-H stretch (CH)
3250	~3286	-	+	+	+	+	+	O-H and N-H stretching vibration (CH)
3390	~3350	-	+	+	+	+	+	DEX and CH interaction
3300-3400	~3370	+	-	+	+	+	+	absorbed water (HAP)
3571	~3571	+	-	-	-	-	-	O-H stretching vibration (HAP)

5.1.2. Cross-linked and double spray dried granules

It was already mentioned that CH has a strong ability to swell (74). In order to improve the drug release the drug delivery system (DDS) was enhanced in the following way: to decrease the negative effect of CH swelling a cross linking agent, glutaraldehyde (GA) was used. Another attempt to improve the DDS was by carrying out a double spray drying step which was envisaged to promote a more effective encapsulation of the drug. The previous research carried out at the laboratory (75) showed that 0,2 wt% of GA is a sufficient amount of GA to cross link CH granules without inducing toxicity of the final product. One of the main requirements for good DDSs is to be non-toxic and not to promote harmful effects to the organism. It is also important that DDS degradation products are also non-toxic compounds to be easily excreted from the body without being accumulated. The components of the DDS studied in the present work are thought to fulfil these requirements.

The morphology of cross linked HAP/CH granules is shown in the Figure 39. There is no significant difference as compared with the previously spray dried granules. As referred by S. G. Véronique Maquet, (76) the cross linking of CH does not change the morphology or size distribution of spray dried CH granules.

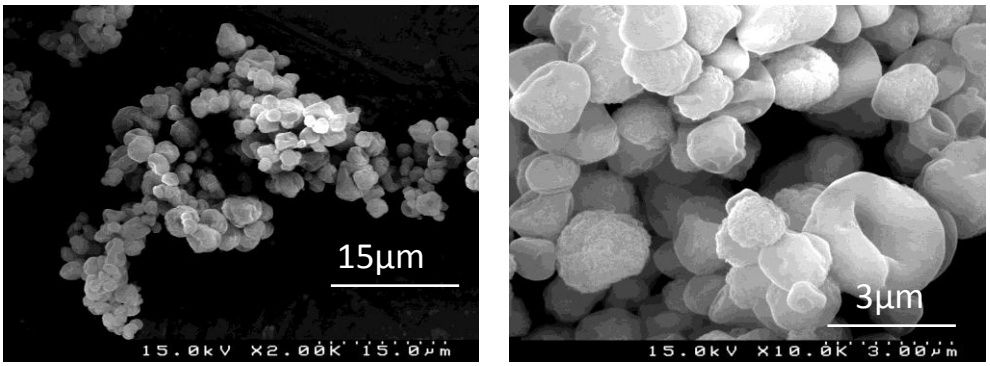

Figure 39 – SEM micrographs of cross linked granules (HAP:CH[1:2]+DEX+0,2GA).

The Figure 40 shows that the granules obtained by double spray drying present a core-shell like structure. The SEM micrographs (Figure 40(a)) illustrate the morphology of HAP+DEX granules produced during the 1st stage of spray drying. The shape and the

surface of these granules are very similar to that of the granules shown in the Figure 34(d). Figure 40(d) presents the SEM micrographs of HAP:CH [1:2]+DEX produced during the 2nd stage of spray drying where a lot of spherical 1,5 – 4 μm granules with a smooth surface are observed. Together with EDS spectrum (Figure 40(d)), that confirms the Ca/P presence, it is possible to make a conclusion that HAP+DEX particles during the 2nd stage of spray drying were covered with a CH layer.

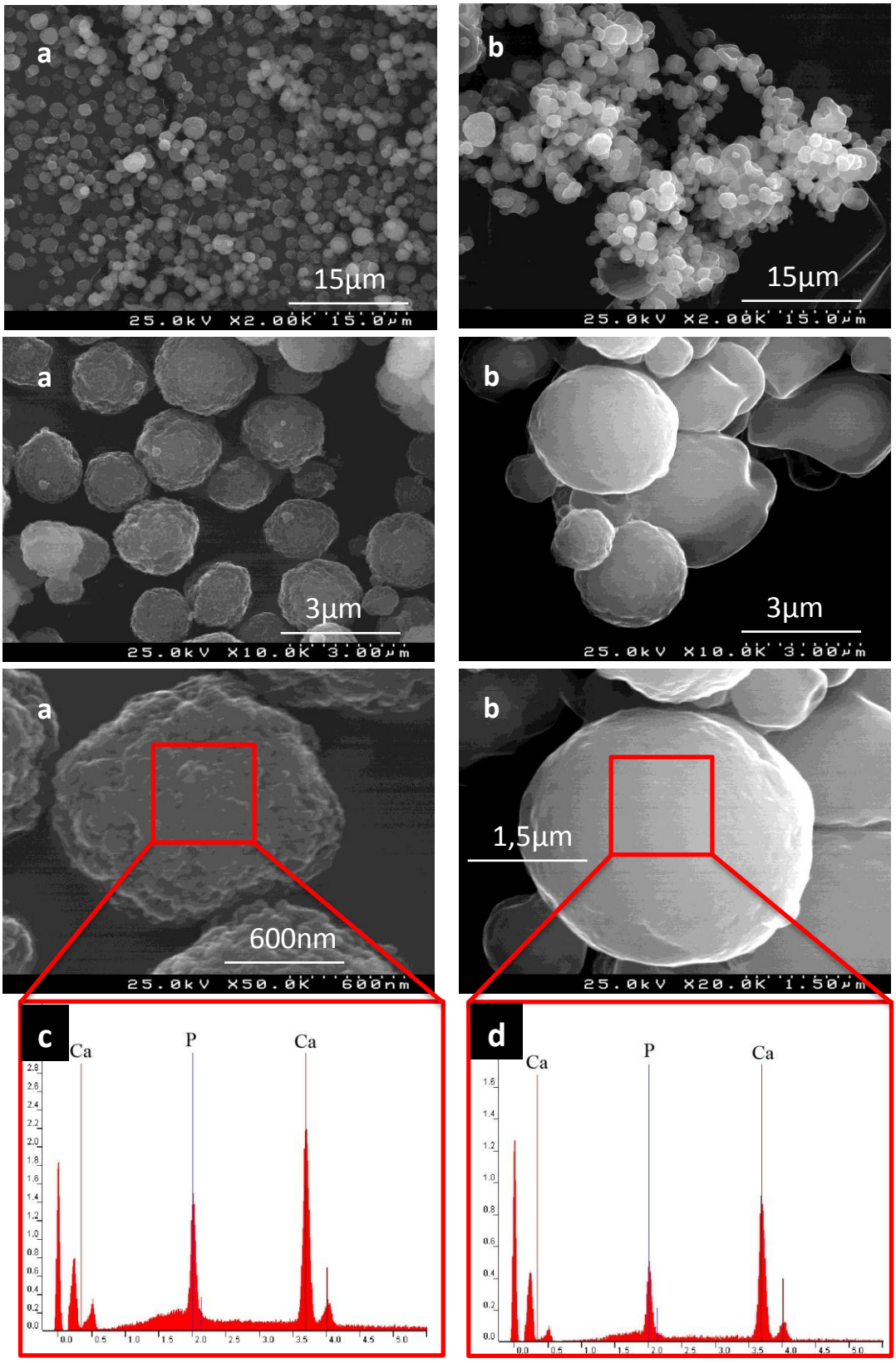

Figure 40 – SEM micrographs and EDS spectra of double spray dried granules: (a) – 1st stage (HAP+DEX); (b) – 2nd stage (HAP:CH [1:2]+DEX); (c) – EDS of HAP+DEX granules; (d) – EDS of HAP:CH [1:2]+DEX granules.

5.2 Drug release experiments

5.2.1 HAP and (HAP: CH) granules

Figure 41 presents the cumulative drug release curves of 3 types of granules, i.e., HAP+DEX granules and composite granules with two different HAP/CH ratios of [1:2] and [2:1]. As observed, in all the cases, the release curve presents an initial burst release followed by a much slower release rate that tends to a plateau where the release has almost stopped. In spite of these common features it may be pointed out that HAP:CH [1:2] presents the faster release as after 8 hours 80% of the drug is already released and the total amount of the DEX becomes released after nearly 50 hours. The other two release profiles which respect the HAP and HAP:CH [2:1] granules reach the plateau later on, i.e. approximately after ~100 hours. The initial fast release of DEX exhibited by the three different types of granules indicates that DEX dissolution from the surface of the drug delivery systems (DDSs) is probably taking place. Also some part of the drug was probably encapsulated inside the granules during spray drying and may account for the slower drug release regime of the curves

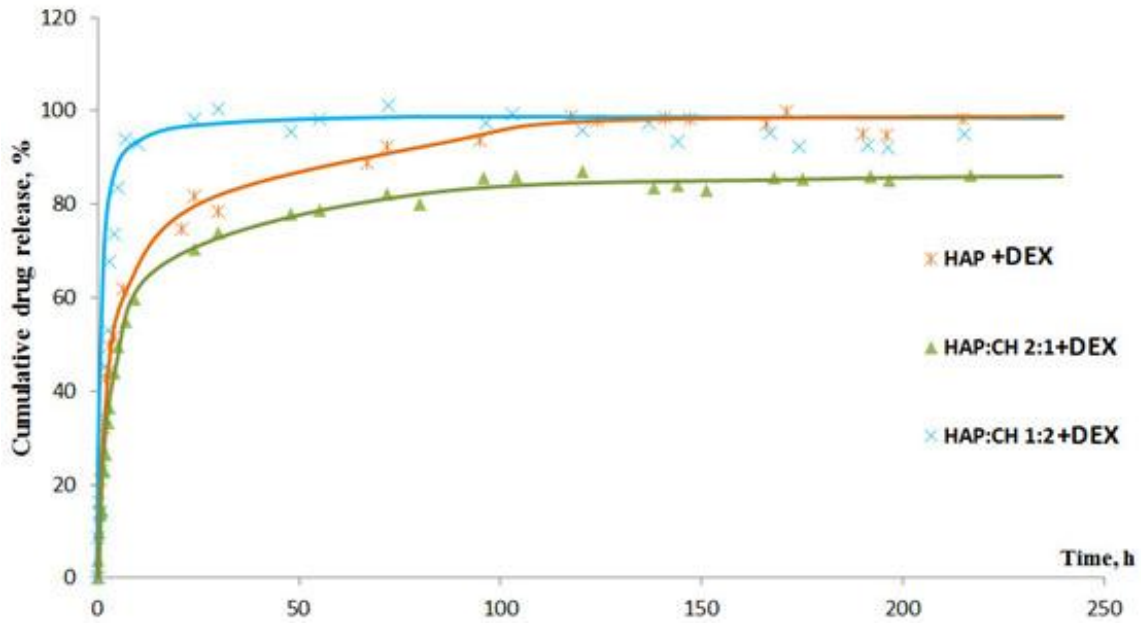

Figure 41 – Cumulative drug release from granules: (Ж) – HAP+DEX; (X) HAP+CH [1:2] +DEX,(▲) – HAP+CH [2:1] +DEX.

As referred previously, the granules HAP:CH [1:2] which have the larger amounts of CH are those with the lower SSA. It may be hypothesized that DEX exists predominantly at the granules surfaces and hence is rapidly released. In the case of the granules HAP

and HAP:CH[2:1] with a larger SSA and hence a larger porosity, it may be considered that the transport of DEX takes place from inner regions of the granules to the release medium and thus is a slower release process than that taking place from a surface region. This reasoning may explain the differences between the profiles of the last granules and that of HAP:CH [1:2] granules.

5.2.2 Cross-linked and double spray dried granules

Figure 42 compares the drug release profiles of composite granules having an HAP:CH ratio equal to [1:2], but produced in different manners: (i) in 1 spray drying stage without additional modification, (ii) cross linked with GA and (iii) in a double spray drying stage. It is observed that as compared to the non-modified granules the release profile from modified granules, i.e. from cross-linked and from double spray dried granules, takes longer to reach a plateau condition. This indicates an overall slower release rate of DEX in the case of the modified granules. For the particular case of cross linked granules and as compared to the non-cross linked system, the amount of released drug after 25 hours was lower, around 20% less. The retarding effect of cross linking in the drug release was also reported in literature: Y.Yan *et al*. (77) have mentioned that increasing the cross-linking degree increases the polymer density and by this way decreases the available free space for drug diffusion. Possibly this effect is also taking place in the cross-linked composite granules where DEX diffusion is made difficult by a denser polymer matrix. The variation of cross-linking degree by using different amounts of various cross-link agents is a promising issue for further studies, since it may open a wide range of possibilities to engineer the drug release rate.

Regarding the release from the double spray dried DDS, it is observed that after an initial fast drug release, which is a typical feature observed in all the other DEX release patterns, a first plateau appears followed then by a second steep release that tends to a new plateau. This behaviour can be interpreted in the following way: the first fast initial release accounts for the DEX existing at the surface of DDS. After the release of the superficial drug amount a plateau occurs indicating that temporarily no drug is available to be released. However prolonging the release time allows the swelling/erosion of the CH surface layer to take place which gives access to the drug encapsulated in the inner region of the granule; because of this a second fast release then occurs which evolves later to a second plateau.

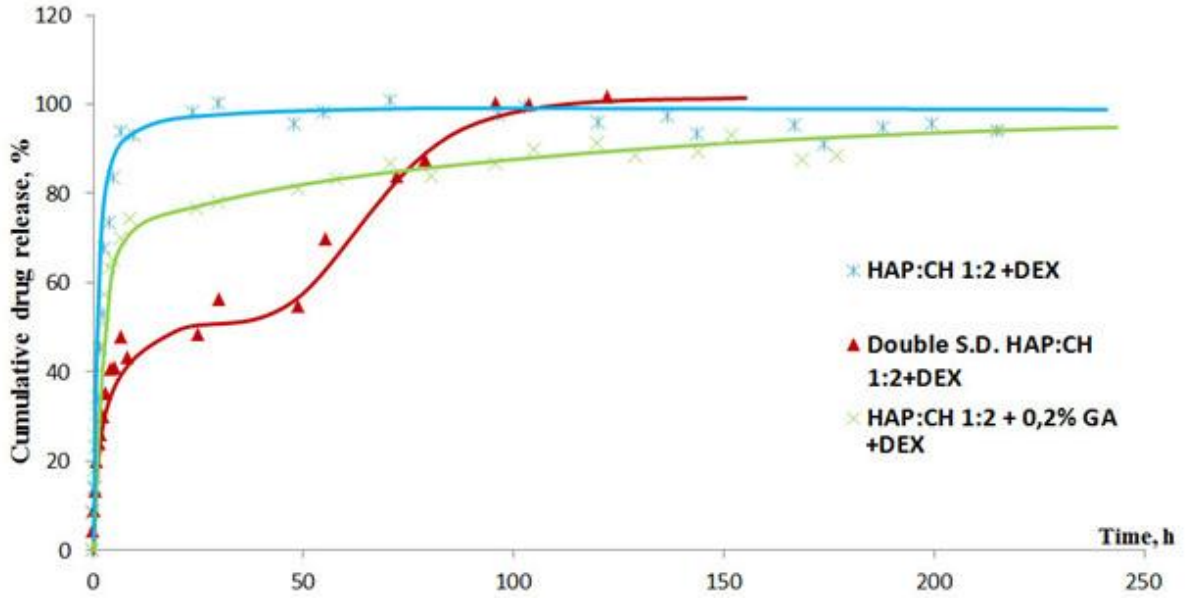

Figure 42 – Cumulative drug release from HAP:CH [1:2]+DEX granules: (✳) – spray dried; (X) cross-linked and spray dried,(▲) – double spray dried.

Analyzing drug release patterns presented above in Figures 41-42, we can conclude that release of DEX can be enhanced by the drug carrier modification (varying ratio of HAP/CH, CH crosslinking, double spray drying). From the therapeutical point of view, HAP:CH[1:2]+DEX granules showed very fast release; after 25 h almost all drug was released. Since the idea of the present work is to study DDS for possible bone treatment applications, robust release is undesirable and attention should be directed to designing DDSs that provide prolonged release. However it is difficult to say why the pattern of HAP+DEX release in Figure 41 falls between that of HAP:CH[1:2]+DEX and HAP:CH[2:1]+DEX. It is possible to assume that the addition of CH disproportionally influence the drug release. Thus, the fastest release was observed for granules with the highest CH concentration. At the same time, HAP:CH[2:1]+DEX granules showed slower release than pure HAP granules loaded with DEX. The positive effect in this case could be explained by the presence of additional layer barrier of CH, which can work in a small manner to reduce the release rate.

Figure 42 shows drug release from the granules with the same HAP/CH ratio [1:2]. This allows analysis of the impact of double spray drying and cross-linking. Since these granules contain around 60 % of CH, it is logical to compare their behavior with pure CH granules. According to the literature review (21-22,45),DDSs of the present work can be

categorized as diffusion-controlled matrix systems. The drug release for such types of DDS strongly depends on the swelling ability of the used polymer (21,45).

In swelling controlled systems, upon particle contact with biological fluid, the polymer starts to swell. Within a short time of liquid penetrating the particle, the glass transition temperature of polymer is lowered due to relaxation of the polymer chains. Drug can diffuse out of the swollen rubber (21).

Figure 42 allows the assumption that, in the studied system, drug release might occur in the same way described above. The fast release from HAP:CH[1:2]+DEX was replaced by more prolonged release for cross-linked granules. And double spray dried granules shows slower release even without cross-linking due to the probability that most of the drug was encapsulated inside the granule. In the outer CH layer the amount of DEX shouldn't be high, since during 2 stage of spray drying in CH solution was immersed HAP+DEX granules. It means that CH can contain only DEX that was released from HAP+DEX microspheres during spray drying.

Comparing the velocity of drug release in this research with (22), in which the drug release from spray dried CH microspheres (size from 2 to 10 μm) was studied, the burst release (less than 30-60 min for the all types of granules for 80-100% drug released) was observed by He et al. This is also attributed with some other papers (78) - spray-dried non-crosslinked CH microparticles loaded with Scopolamine hydrobromide showed complete release after 1,5-2 hours. In both studies (22) and (78) there was mentioned that cross-linking allows to slightly slow down release. All these are correlated with the results of this research. Moreover, it helps to explain longer release observed in Figures 41-42. Slower release from HAP/CH in comparison with the above mentioned releases for CH microspheres can be explained by the use of HAP. Taking into consideration all that was mentioned above the usage of HAP and CH allows to produce DDS with more prolonged time of drug release than when these components where used separately. Moreover, core-shell structure cross-linking and structuring showed good results for further improvement of drug release.

5.2.3 Granules degradation during drug release

To analyse the influence of PBS solution during the drug release experiment SEM micrographs of granules before immersing into PBS (Figure 43(1-2)) and after 24 h staying in PBS solution (Figure 43(3-4)) were compared. It is possible to observe that HAP+DEX granules maintained their shape. A little change in the surface, which looks

more rough as compared to the initial granules, can be explained by washing-out of small HAP particles during sample washing (washing was done to avoid the presence of crystals of the salts from PBS solution). Composite HAP:CH[1:2]+DEX and HAP:CH[2:1]+DEX granules show significant morphology changes. It is clear that the polymer after the drug release experiment did not maintain its original shape. This behaviour can be explained by the high swelling ability of CH.

The morphology of double spray dried and cross-linked granules after 5 days release in PBS solution is shown in Figure 44. It may be observed that the changes in granules morphology are similar to the one observed in Figure 43. While the role of crosslinking cannot be observed in the SEM images alone, as the particle morphologies remain similar to those seen in Figure 43, the beneficial effect of crosslinking can be observed in Figure 42 showing the drug release curves. It was not observed the difference in morphology for cross-linked granules. However, the positive effect of was shown in Figure 42, where it clear that cross-linking allows to slow down drug release. Because of its swelling properties, CH does not maintain its morphology through the drug release process. The HAP particles, on the other hand, keep their structural properties.

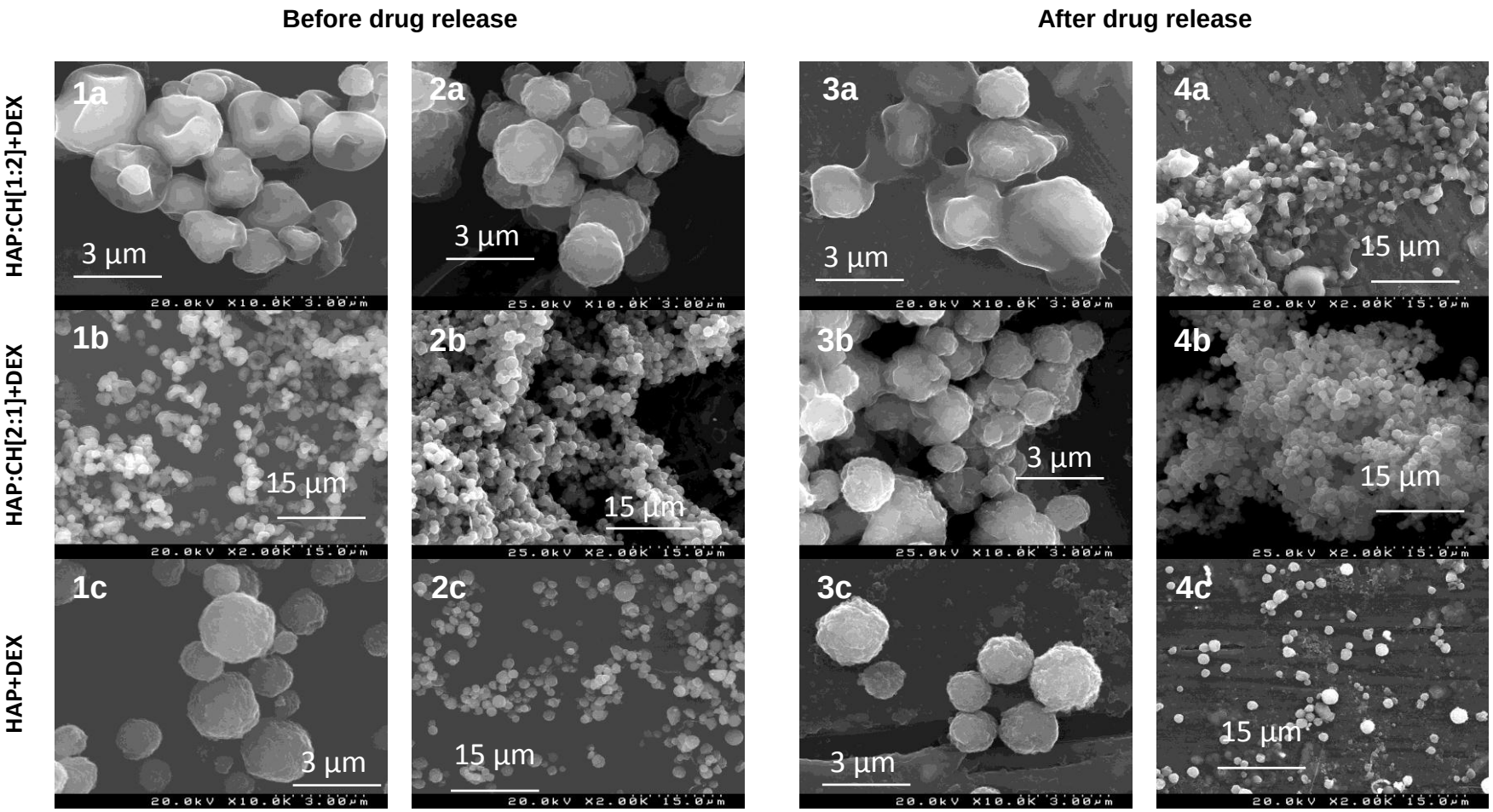

Figure 43 – Granules morphology before (1-2) and after (3-4) drug release experiment (24h): (a) – HAP:CH [1:2] +DEX;(b) – HAP:CH [2:1] +DEX; (c) – HAP +DEX

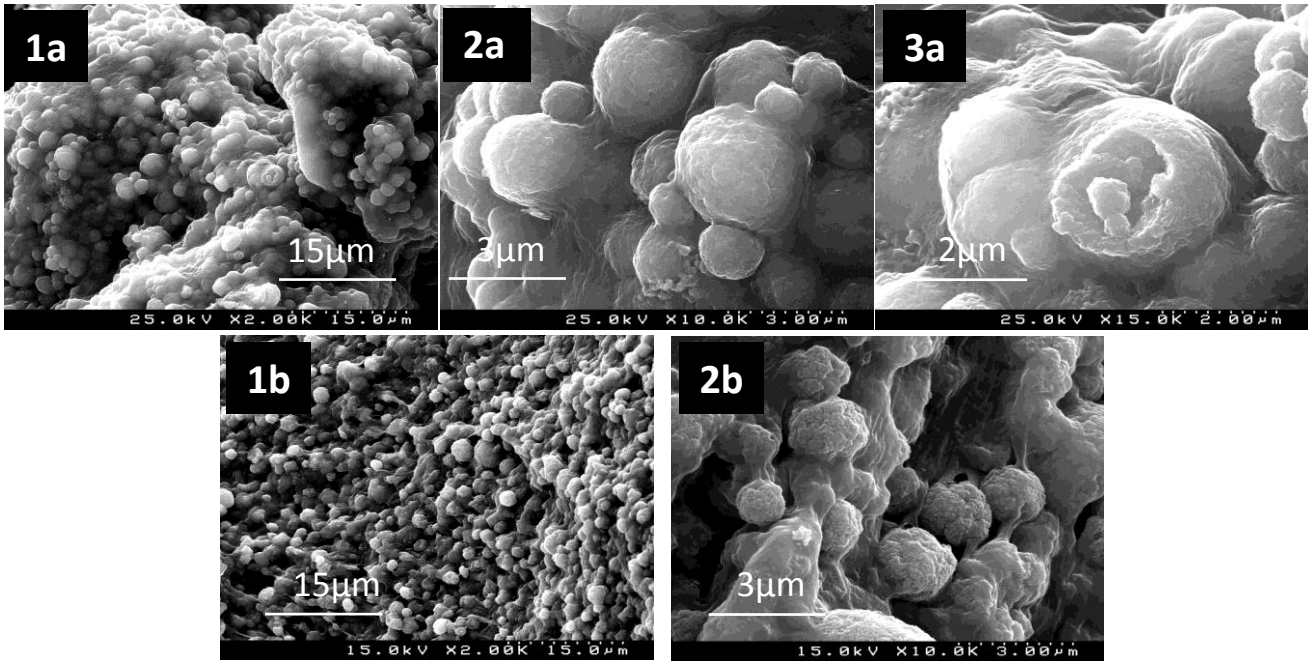

Figure 44 – SEM micrographs of granules after 5 days of drug release experimente: (a) – double spray dried (HAP:CH[1:2]+DEX) and (b) – cross linked (HAP:CH[1:2]+DEX+0,2GA).

5.2.4 Identification of the appropriate mathematical model

Selecting an appropriate mathematical model to describe the drug release profile may allow to predict the effect of DDS modification (morphology composition of the granules) and to elucidate the mechanisms involved in the drug release process. In the following chapter four mathematical models were compared with the experimental drug release data. The evaluation of the convergence between the experimental data and the mathematical models was undertaken by comparing the $R^2_{adj.}$ fitting coefficient (Figure 46). The models where chosen based on their main features which are summarized in Table 8.

Table 8 – Mathematical models selected for fitting the experimental DEX release data points.

Mathematical model	**Equation**	**Main features of the model**
Higuchi	F=kH*t^0.5	- the 1st mathematical model used for drug release; - simple model; - is“starting point” for many other models (79)
Hixson-Crowell	F=100*[1-(1-kHC*t)^3]	indicated for :

		- spherical particles, which shape doesn't change with time; - particles that remain intact and do not disintegrate into smaller fragments during dissolution
Peppas-Shalin	F=k1*t^m+k2*t^(2*m)	- water penetrates in the polymer matrix and the polymer swelling takes place; - swelling creates a rubbery region, in which the drug diffusivity increases substantially. -during the swelling, two different states occur: the glassy core and the gel layer (rubbery), exist in the polymer matrix
Weibull	F=Fmax*{1-Exp[-(t^β)/α]}	- empirical model

The Hixson-Crowell model was selected because it is recommended for spherical particles that maintain a stable morphology; this is the case of HAP+DEX granules which keep a constant spherical shape throughout the release period as previously referred and documented by Figure 43(c). Peppas model one of the commonly used for diffusion-controlled systems (21).

Weibull is an empirical model which was created to fit mathematically to the drug release curves regardless the nature of the DDS. And Higuchi model was chosen for comparison, as it is a simple model appropriate to describe a simple release process based on diffusion.

The fitting of the various models to the different release curves was assisted by the software DDsolver. Figure 45 illustrates the fitting results respecting the (HAP+DEX) granules.

Figure 46 compares the fitting parameter corresponding to the various DDSs and marthematical models under analysis. It is obvious that Weibul and Peppas-Shalin model fit very well to all the drug release profiles with a fitting coefficient close to one. Higuchi model in spite of its simplicity does not apply to many of the DDSs; its best fit was obtained with the double spray dried granules. The poor result of Hixson-Crowell is correlated with Figures 43-44, since in Table 8 it is mentioned that this model describes DDSs wich spherical particles and size are staying the same during drug release.

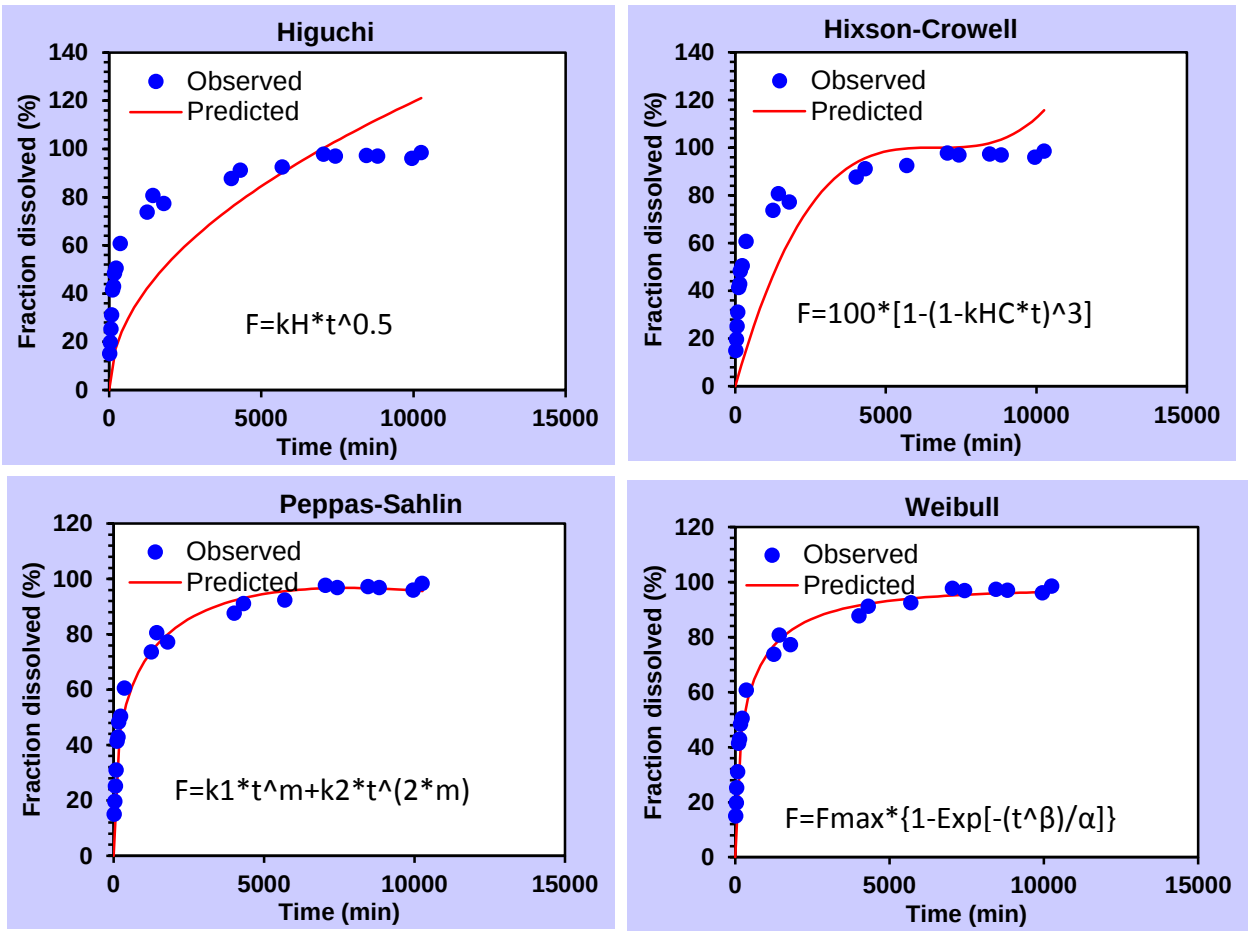

Figure 45 – Comparison of theoretical mathematical model with experimental drug release data for HAP+DEX made with DDsolver.

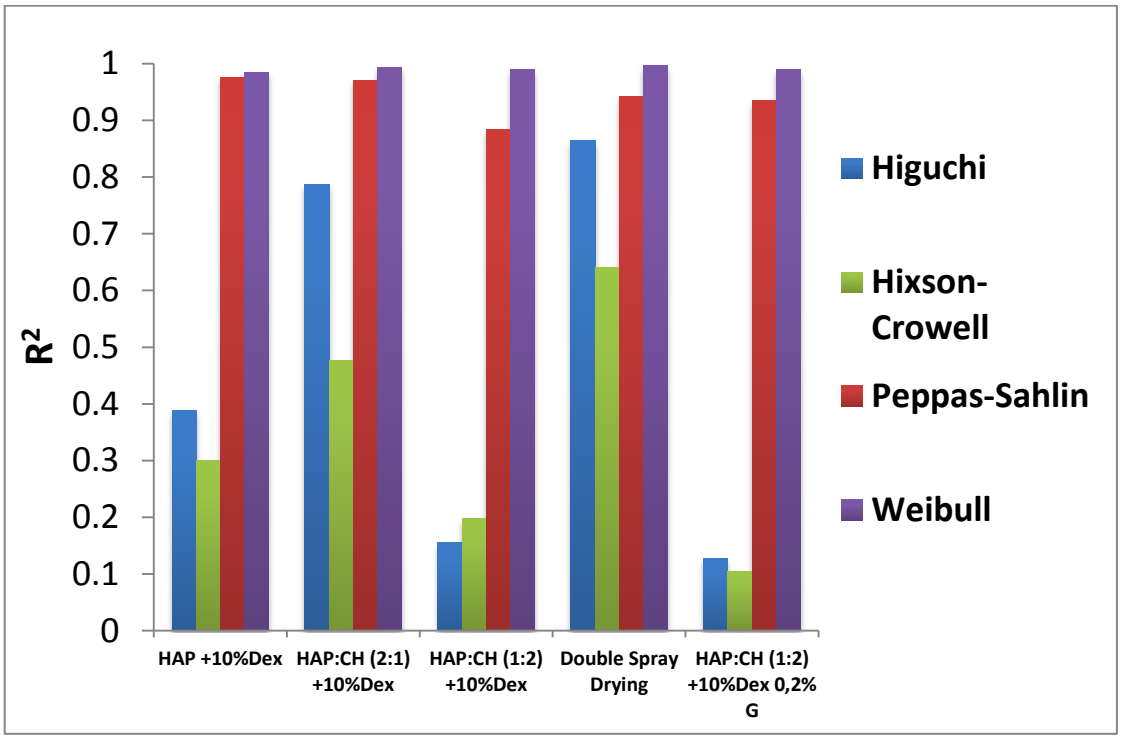

Figure 46 – Comparison of models appropriating to experimental data.

As it was shown by SEM analysis the size and morphology of DDS in present work was different after the drug release.

Good fitting of Weibull model was expected, since it is empirical model. This model doesn't have any parameter related with the intrinsic dissolution rate of the drug and there is no any y kinetic fundament. Weibull model can only describe, but doesn't characterize the system (26). As it is mentioned by V. Papadopoulou in (80) that Weibul function can be used for kinetic release from a variety of DDSs, but it cannot "provide a hint for the release mechanisms of the drug in relation to the estimates of the Weibull parameters". Shows one more time that Weibull model is appropriate for describing drug release, but not for identification the release mechanism, for example. However V. Papadopoulou in his work (80) was able to find some links between the values of empirical model constants and the diffusional mechanisms of the release.

The main conclusion of so well fitting Peppas-Shalin model to obtained drug release patterns, proves one more time that assumption made after drug release curves were analysed is correct. The HAP/CH DDSs in present work be categorized as diffusion-controlled systems and the drug release should be very similar and conform to the mechanisms described in this paper in 2.1.2.

The choice of a mathematical model for developing DDS elucidating drug release mechanisms depends on the desired or required predictive ability and accuracy of the model. Sometimes the use of a simple empirical or semi-empirical model can be absolutely sufficient. However, when reliable, detailed information are required, more complex, mechanistic theories must be applied (81).

Chapter 6

Conclusions and Recommendations

6. Conclusions and Recommendations

This research studies the potential of HAP/CH microgranules for use in drug (DEX) incorporation and subsequent application as controlled release systems for this drug. The effects of the following parameters of granules preparation on the drug release behaviour were analysed:

- the variation of HAP/CH ratio;
- the effect of polymer crosslinking;
- the effect of double spray drying;

At the end of the work the obtained results were compared with different mathematical models and the best model was fitted to each composition of the DDS under study.

The main conclusions withdrawn from the results obtained throughout this research can be summarized as follows:

- Spray drying is a convenient technique for producing micro-sized composite (HAP/CH) granules. It allows getting homogeneous granules with controllable morphology.
- The granules spray dried from the suspensions with different ratios of HAP/CH have different morphology. With increasing CH ratio the shape changes from the spherical granules with rough surface to particles with concavities and smooth surface.
- Granules with *CH:HAP [2:1]+DEX* composition showed the most robust drug release (after 7h almost 80% of DEX was released) among all the *other* studied type of granules.
- The cross-linking of CH has positive effect on drug release, Addition of 0,2 % of GA allowed to slow down the release of the drug. Due to the high swelling ability of CH it is necessary to use cross-link agents to prolong the drug release.
- Double spray drying allowed producing core-shell structured granules, which showed even more prolonged DEX release. The two stepped release profile was observed, what can be explaining by the robust release of the drug from the surface during the 1st step and the following release of the drug from the internal part of the granules. From the results obtained when adjusting few mathematical models to the modulation of the results, it can be concluded that Peppas-Shalin and Weibull models are the most appropriate models for describing drug release for the all studied compositions of DDS.

- The results of drug release and mathematical modelling showed that HAP/CH DDS in present work can be attributed to diffusion-controlled systems.

Recommendations for future work

The results obtained in the present work revealed some needs of further studies aiming to clarify the following issues:

1. The evaluation of the drug distribution DDS may help better understand the mechanisms involved into the drug release and as a result the release can be controlled better. For the determination of DEX distribution in the solid state Dexamethasone Fluorescein (82) can be used with further Fluorescence Lifetime Imaging (FLIM) analysis or observation under a fluorescence microscope. (39)
2. This research showed that producing core-shell structured granules by double-spray drying is very sensitive to minor variations of the experimental conditions and thus require be repeating and studying in more detail.
3. There is new generation of spray dryers (Mini Spray Dryer B-290 (83)) with 3-fluids nozzles instead of 2-fluids, what allows producing core shell structured granules in one stage with high practical yield. Usage of such type of nozzles allows producing granules from two different solutions at the same time. Thus core-shell particles can be spray dried (there is even possibility to produce liquid core). The variation of feeding rates of two suspensions makes it possible to regulate thickness of the shell layer or the size of the core part;(85-86)
4. The further studying of the influence of the amount of the cross link agent on the drug release should be done. Different types of cross link agents might be used in experiment: low-toxic and natural compounds such as Genipin (77), TPP (86), etc.
5. Since the pH at the nidus of inflammation might be different from the neutral, the drug release in buffer solutions with different pH (close to possible physiologic one) and the study of influence of pH on drug release rate should be carried out.
6. Differential pulse voltammetry (DPV) and Square-wave adsorptive voltammetry (SW-AdsV) techniques can be used instead of UV-vis spectroscopy for the evaluation of released DEX. The advantages of these methods are: high detection ($7.6 \cdot 10^{-6}$ mol/L and $2.54 \cdot 10^{-9}$ mol/L) and quantification limits ($8.47 \cdot 10^{-9}$ mol/L); no need of taking different samples through different time interval – it allows to check the change of DEX concentration online. In both techniques hanging mercury drop electrode (HMDE) is used as the working electrode, Ag/AgCl as references electrode and platinum (for DVP) or graphite rode (for

SW-AdsV) as auxiliary electrode. Previously deaerated with nitrogen solution of DEX is cathodic scanned. The obtained polarogram (a plot of current against potential) contains oxidation/reduction loop with characteristic peaks. The intensity of these peaks is attributed to DEX concentration in the solution (87) (88).

7. Biocompatibility test of researched DDS should be carried out in order to study the cell response.

References

1. **Y. Pathak, D. Thassu.** *Drug delivery nanoparticles formulation and characterization.* New York : Informa Healthcare USA, Inc., 2009.

2. **http://www.bccresearch.com/market-research/pharmaceuticals/advanced-drug-delivery-systems-phm006h.html.** Advanced Drug Delivery Systems: Technologies and Global Markets. Access: April, 2014.

3. **H. Hirabayashi, J. Fujisaki.** Bone-Specific Drug Delivery Systems. *Clinical Pharmacokinetics.* 2003, Vol. 42, pp. 1319-1330.

4. **K.J. Kewal.** *Drug Delivery Systems.* Basel, Switzerland : Humana Press, 2008.

5. **K. Dash, G.C. Cudworth.** Therapeutic applications of implantable drug delivery systems. *Journal of Pharmacological and Toxicological Methods.* 1998, Vol. 40, 1, pp. 1-12.

6. **A.K. Bajpai, S.K. Shukla, S. Bhanu, S. Kankane.** Responsive polymers in controlled drug delivery. *Progress in Polymer Science.* 2008, Vol. 33, 11, pp. 1088-1118.

7. **S. Ekins, J. J. Xu.** *Drug Efficacy, Safety, and Biologics Discovery: Emerging Technologies and Tools.* s.l. : John Wiley & Sons, 2009. pp. 3-75.

8. **S.J. Rayan.** *RETINA.* s.l. : Elsevier, 2013. pp. 693-694.

9. **J. Gong, M. Chen, Y. Zheng, S. Wang, Y. Wang.** Polymeric micelles drug delivery system in oncology. *Journal of Controlled Release.* 2012, Vol. 159, 3, pp. 312–323.

10. **W. Xu, P. Ling, T. Zhang.** Polymeric Micelles, a Promising Drug Delivery System to Enhance Bioavailability of Poorly Water-Soluble Drugs. *Journal of Drug Delivery.* 2013, pp. 1-15.

11. **T.M. Allena, P.R. Cullis.** Liposomal drug delivery systems: From concept to clinical applications. *Advanced Drug Delivery Reviews.* 2013, Vol. 65, 1, pp. 36–48.

12. **P. Kesharwani, K.Jain , N. Jain.** Dendrimer as nanocarrier for drug delivery. *Progress in Polymer Science.* 2014, Vol. 39, 2, pp. 268–307.

13. **A.R. Menjogea, A.L. Rinderknechtc, R.S. Navatha, M.Faridniac, C.J. Kimb, R. Romerob, R.M. Kannan.** Transfer of PAMAM dendrimers across human placenta: Prospects of its use as drug carrier during pregnancy. *Journal of Controlled Release.* 2011, Vol. 150, 3, pp. 326–338.

14. **A.G. Cuenca, H. Jiang, S. N. Hochwald, M. Delano, W. G. Cance.** Emerging Implications of Nanotechnology on Cancer Diagnostics and Therapeutics. *Cancer.* 2006, Vol. 107, 3, pp. 459–466.

15. **V.V. Mody, A. Cox, S. Shah, A. Singh, W. Bevins, H. Parihar.** Magnetic nanoparticle drug delivery systems for targeting tumour. *Applied Nanoscience.* 2014, Vol. 4, 4, pp. 385-392.

16. **N. Dixit, S.D. Maurya, B.P.S.Sagar.** Sustained Release Drug Delivery System. *Indian Journal of Research in Pharmacy and Biotechnology.* 2013, Vol. 1, 3, pp. 305-310.

17. **T Hickeya, D Kreutzerb, D.J Burgessc, F Moussy.** Dexamethasone/PLGA microspheres for continuous delivery of an anti-inflammatory drug for implantable medical devices. *Biomaterials.* 2002, Vol. 23, 7, pp. 1649–1656.

18. **http://www.slideshare.net/gajendragupta75491/microspheres-as-drug-delivery-system.** Microspheres as drug delivery system. Access: July, 2014.

19. **J.H. Park, M. Ye, K. Park.** Biodegradable Polymers for Microencapsulation of Drugs. *Molecules.* 2005, Vol. 10, pp. 146-161.

20. **M. C. Sunny, P. Ramesh, H. K. Varma.** Microstructured microspheres of hydroxyapatite bioceramic. *Journal of Materials Science: Materials in Medicine.* 2002, Vol. 13, 7, pp. 623-632.

21. **S.A. Agnihotri, N. N. Mallikarjuna, T. M. Aminabhavi.** Recent advances on chitosan-based micro- and nanoparticles in drug delivery. *Journal of Controlled Release.* 2004, Vol. 100, pp. 5-28.

22. **P. He, S.S. Davisa, L. Illum.** Chitosan microspheres prepared by spray drying. *International Journal of Pharmaceutics.* 1999, Vol. 187, 1, pp. 53–65.

23. **S. Dash, P.N. Murthy, L. Nath.** Kinetic modelling on drug release from controlled drug delivery systems. *Acta poloniae pharmaceutica.* 2010, Vol. 67, pp. 217-223.

24. **J. Siepmann, N.A. Peppas.** Modeling of drug release from delivery systems based on hydroxypropyl methylcellulose (HPMC). *Advanced Drug Delivery Reviews.* 2001, Vol. 48, pp. 139-157.

25. **D.R. Paul.** Elaborations on the Higuchi model for drug delivery. *International Journal of Pharmaceutics.* 2011, Vol. 418, pp. 13-17.

26. **P. Costa, J. M.S. Lobo.** Modeling and comparison of dissolution profiles. *European Journal of Pharmaceutical Sciences.* 2001, Vol. 13, pp. 123-133.

27. **G. Singhvi, M. Singh.** Review: In-Vitro Drug Release Characterization Models. *International Journal of Pharmaceutical Studies and Research.* 2011, Vol. 2, pp. 77-84.

28. **D.Y. Arifina, L.Y. Leea, C.H. Wang.** Mathematical modeling and simulation of drug release from microspheres: Implications to drug delivery systems. *Advanced drug delivery reviews.* 2006, Vol. 58, 12-13, pp. 1274-325.

29. **A.S. Mistry, A.G. Mikos.** Tissue Engineering Strategies for Bone Regeneration. *Advances in Biochemical Engineering.* 2005, 94, pp. 1-22.

30. **K. Fox, P.A. Tran, N. Tran.** Recent advances in research applications of nanophase hydroxyapatite. *ChemPhysChem.* 2012, Vol. 13, 10, pp. 2495-506.

31. **L. Pighinelli, M. Kucharska.** Chitosan-hydroxyapatite composites. *Carbohydrate Polymers.* 2013, Vol. 93, pp. 256-62.

32. **V. Uskoković, D.P. Uskoković.** Nanosized hydroxyapatite and other calcium phosphates: chemistry of formation and application as drug and gene delivery agents. *Journal of Biomedical Materials Research Part B: Applied Biomaterials.* 2011, Vol. 96, pp. 152-91.

33. **M.H. Fathi, A. Hanifi, V. Mortazavi.** Preparation and bioactivity evaluation of bone-like hydroxyapatite nanopowder. *Journal of Materials Processing Technology.* 2008, Vol. 202, 1-3, pp. 536-542.

34. **M.A. Martins, C. Santos, M.M. Almeida, M.E.V. Costa.** Hydroxyapatite micro- and nanoparticles : Nucleation and growth mechanisms in the presence of citrate species. *Journal of Colloid and Interface Science.* 2008, Vols. 210–216, pp. 210–216.

35. **A.K. Nayak.** Hydroxyapatite Synthesis Methodologies: An Overview. *International Journal of ChemTech Research.* 2010, Vol. 2, 2, pp. 903-907.

36. **K. L. Aw, W. H. Yeo, C. Y. Tan, S. Ramesh, I. Sopyan, M. Hamdi.** Consolidation of Nanocrystalline Hydroxyapatite Powder for Medical Applications. *ICCBT - F.* 2008, Vol. 17, pp. 171-180 .

37. **Y. Shinto, A. Uchida, F. Korkusuz, N. Araki, K. Ono.** Calcium hydroxyapatite ceramic used as a delivery system for antibiotics. *Britsh Editorial Society of Bone and Joint Surgery.* 1992, Vol. 74, pp. 600-604.

38. **F. Croisier, C. Jérôme.** Chitosan-based biomaterials for tissue engineering. *European Polymer Journal.* 2013, Vol. 49, pp. 780-792.

39. **T.R Seda, A.C. Abdullah, G. Menemşe, N.M. Rahime.** In vitro release of dexamethasone or bFGF from chitosan/hydroxyapatite scaffolds. *Journal of Biomaterials Science, Polymer Edition.* 2009, Vol. 20, 13, pp. 1899-1914.

40. **http://www.aoxing-biology.com/images/pro-c-2-1_clip_image002.jpg.** Access: June, 2014.

41. **A. Bernkop-Schnürch, S. Dünnhaupt.** Chitosan-based drug delivery systems. *European Journal of Pharmaceutics and Biopharmaceutics.* 2012, Vol. 3, 81, pp. 463-469.

42. **O.A.C. Monteiro, C. Airoldi.** Some studies of crosslinking chitosan–glutaraldehyde interaction. *International Journal of Biological Macromolecules.* 1999, Vol. 26, pp. 119–128.

43. **D.J. Macquarrie, A. Bacheva.** Efficient subtilisin immobilization in chitosan, and peptide synthesis using chitosan–subtilisin biocatalytic films. *Green Chemistry.* 10, 2008, 6, pp. 692–695.

44. **http://www.ag.kagawa-u.ac.jp/foodeng.yoshii/TWA.pdf.** Particle Technology & Chemical Engineering Units for Food & Pharmaceutical Applications. Access: June, 2014.

45. **T.A. Sonia, C.P. Sharma.** Chitosan and its derivatives for drug delivery perspectives. *Advances in Polymer Science.* 2011, Vol. 243, pp. 23-54.

46. **http://www.cancer.org/treatment/treatmentsandsideeffects/guidetocancerdrugs/dexamethasone.** Dexamethasone. Access: June, 2014.

47. **M.C.T. Cabral, M.A. Costa, M.H. Fernandes.** In vitro models of periodontal cells: a comparative study of long-term gingival, periodontal ligament and alveolar bone cell cultures in the presence of b-glycerophosphate and dexamethasone. *Journal of Materials Science: Materials in Medicine.* 2007, 18, pp. 1079–1088.

48. **C.F. Lacy, L.L. Armstrong, M. Goldman.** *Drug information handbook.* s.l. : Lexi-Comp, 2009. pp. 2039-2048.

49. **https://www.sigmaaldrich.com/content/dam/sigma-aldrich/docs/Sigma/Datasheet/3/d6645dat.pdf.** Dexamethasone SIGMA Reference Standart. *Access: June, 2014.*

50. **http://img.guidechem.com/mdsd/50-02-2_1289302204890.pdf.** Organics, ACROS. *Material Safety Data Sheet, Dexamethasone, 96%.* Access: July, 2014.

51. **T. Gale.** *The Gale Encyclopedia Of Cancer: A Guide To Cancer And Its Treatments.* s.l. : Gale / Cengage Learning, 2005.

52. **N.J.S. London, A. Chiang, J.A. Haller.** The Dexamethasone Drug Delivery System: Indications and evidence. *Advances in Therapy.* 2011, Vol. 28, 5, pp. 351-366.

53. **S.S. Jun, M. Appleford, J.L. Ong, J.C. Wenke, J.M. Kim, S.H. Choi, D.S. Oh.** Porous hydroxyapatite scaffold with three-dimensional localized drug delivery system using biodegradable microspheres. *Journal of Controlled Release.* 2011, Vol. 153, pp. 133–140.

54. **http://www.lagep.cpe.fr/wwwlagep7/en/atomiseur-de-laboratoire-buchi-b-191/.** Access: June, 2014.

55. **http://s.hswstatic.com/gif/scanning-elecron-microscope-illustration.jpg.** How Scanning Electron Microscopes Work. Access: March, 2014.

56. **B. H. Stuart.** *Infrared Spectroscopy: Fundamentals and Applications.* Fundamentals and Applications : Willey, 2004.

57. **http://en.wikipedia.org/wiki/Fourier_transform_infrared_spectroscopy.** Fourier transform infrared spectroscopy. Access: June, 2014.

58. **F.A. Settle.** *Handbook of Instrumental Techniques for Analytical Chemistry.* Cloth : Prentice Hall, 1997.

59. **А. Егоров.** *ИНФРАКРАСНАЯ ФУРЬЕ-СПЕКТРОСКОПИЯ.Электронное учебно-методическое пособие.* Нижний Новгород : Нижегородский госуниверситет, 2012. (A.Egorov, Fourier Transform Infrared Spectroscopy. Manual for students. Nizhny Novgorod, Nizhny Novgorod University, 2012).

60. **A.R. Barron, N. Hwang.** BET Surface Area Analysis of Nanoparticles. [book auth.] A.R. Barron. *Physical Methods in Chemistry and Nano Science.* 2011.

61. **F. Rojas, I. Kornhauser, C. Felipe, J. M. Esparza, S. Cordero, A. Domıngueza, J. L. Riccardo.** Capillary condensation in heterogeneous mesoporous networks consisting of variable connectivity

and pore-size correlation. *Physical Chemistry Chemical Physics.* 30 04 2002, Vol. 4, 11, pp. 2346–2355.

62. **M. Thommes.** Physical Adsorption Characterization of Nanoporous Materials. *Chemie Ingenieur Technik.* 2010, Vol. 82, 7, p. 1059.

63. **http://upload.wikimedia.org/wikipedia/commons/thumb/9/95/Schematic_of_UV-_visible_spectrophotometer.png/800px-Schematic_of_UV-_visible_spectrophotometer.png.** Ultraviolet–visible spectroscopy. Access: May, 2014.

64. **J. Räty, K.E. Peiponen, T. Asakura.** *UV-Visible Reflection Spectroscopy of Liquids.* Berlin : Springer, 2004.

65. **A.L.V. Pires.** Sistemas compósitos de PU/ZnO para entrega de fármacos. *Master Thesis, University of Aveiro.* 2012.

66. **Y. Zhang, M. Huo, J. Zhou, A. Zou, W. Li, C. Yao,.** DDSolver: An Add-In Program for Modeling and Comparison of Drug Dissolution Profiles. *The American Association of Pharmaceutical Scientists Journal.* 2010, Vol. 12, 3, pp. 263–271.

67. **V. Mohanasrinivasan, Mudit Mishra, Jeny Singh Paliwal, Suneet Kr. Singh, E. Selvarajan , V. Suganthi, C. Subathra Devi.** Studies on heavy metal removal efficiency and antibacterial activity of chitosan prepared from shrimp shell waste. *3 Biotech.* 2014, Vol. 4, 2, pp. 167–175.

68. **http://webbook.nist.gov/cgi/cbook.cgi?ID=C50022&Mask=80#IR-Spec.** Dexamethasone. Access: June, 2014.

69. **S.M. Maisara, P. Arsad, M.Lee.** Synthesis and Characterization of Hydroxyapatite Nanoparticles. *2nd International Conference on Biotechnology and Food Science.* 2011, Vol. 7, pp. 184 - 188.

70. **A. Wang, D. Liu, H. Yin, H. Wu, Y. Wada, M. Ren, T. Jiang, X. Cheng, Y. Xu.** Size-controlled synthesis of hydroxyapatite nanorods by chemical precipitation in the presence of organic modifiers. *Materials Science and Engineering: C.* 2007, Vol. 27, pp. 865-869.

71. **G. Lawrie, I. Keen, B. Drew, A. Chandler-Temple, L. Rintoul, P. Fredericks, L. Grøndahl.** Interactions between Alginate and Chitosan Biopolymers Characterized Using FTIR and XPS. *Biomacromolecules.* 2007, Vol. 8, pp. 2533-2541.

72. **L.L. Fernandes, C.X. Resende, D.S. Tavares, G.A. Soares.** Cytocompatibility of Chitosan and Collagen-Chitosan Scaffolds for Tissue Engineering. *Polímeros.* 2011, Vol. 21, 1, pp. 1-6.

73. **L.B. Rodriguesa, H.F. Leitea, M.I. Yoshidab, J.B. Salibaa, A.S. Juniora, A.G. Faraco.** In vitro release and characterization of chitosan films as dexamethasone carrier. *International Journal of Pharmaceutics.* 2009, Vol. 368, pp. 1-6.

74. **L. Pighinelli, M. Kucharska.** Chitosan-hydroxyapatite composites. *Carbohydrate polymers.* 2013, Vol. 93, 1, pp. 256-62.

75. **F.R.V. Pinto.** Citocompatibilidade de matrizes de quitosano/fosfato de cálcio. *Master Thesis, University of Aveiro.* December 2013.

76. **http://www.sigmaaldrich.com/materials-science/polymer-science/chitosan.html.** V. Maquet, S. Gautier. *Preparation of Chitosan Microparticles by Spray Drying.* Access: May, 2014.

77. **Y.Yuan, B.M.Chesnutt, G.Utturkar, W.O. Haggard, Y.Yang, J.L.Ong, J.D.Bumgardner.** The effect of cross-linking of chitosan microspheres with genipin on protein release. *Carbohydrate Polymers.* 2007, Vol. 68, pp. 561–567.

78. **F.Q. Li, C. Yan, J. Bi, R.R. Ji, X. Chen, J.C. Su, J.H. Hu.** A novel spray-dried nanoparticles-in-microparticles system for formulating scopolamine hydrobromide into orally disintegrating tablets. *International Journal of Nanomedicine.* 2011, Vol. 6, pp. 897–904.

79. **J. Siepmann, F. Siepmann.** Modelling of diffusion controlled drug delivery. *Journal of controlled releas.* 2012, Vol. 161, pp. 351-62.

80. **V. Papadopouloua, K. Kosmidisb, M. Vlachoua, P. Macheras.** On the use of the Weibull function for the discernment of drug release mechanisms. *International Journal of Pharmaceutics.* 2006, Vol. 309, 1-2, pp. 44–50.

81. **J. Siepmann, N.A Peppas.** Modeling of drug release from delivery systems based on hydroxypropyl methylcellulose (HPMC). *Advanced drug delivery reviews.* 2001, Vol. 48, pp. 139–157.

82. **http://www.lifetechnologies.com/order/catalog/product/D1383.** lifetechnologies. Access: June, 2014.

83. **http://www.buchi.com/en/products/spray-drying-and-encapsulation/mini-spray-dryer-b-290.** Mini Spray Dryer B-290. Access:June, 2014.

84. **V. Tokárová, O. Kašpar, Z. Knejzlík, P. Ulbrich, F. Štěpánek.** Development of spray-dried chitosan microcarriers for nanoparticle delivery. *Powder Technology.* 2013, 235, pp. 797–805.

85. **O. Kašpar, M. Jakubec, F. Štěpánek.** Characterization of spray dried chitosan–TPP microparticles formed by two- and three-fluid nozzles. *Powder Technology.* 2013, 240, pp. 31–40.

86. **X.Z. Shu, K.J. Zhu.** A novel approach to prepare tripolyphosphate/chitosan complex beads for controlled release drug delivery. *International journal of pharmacutics.* 2000, Vol. 201, pp. 51-58.

87. **I. Baranowskaa, P. Markowskia, A. Gerlea, J. Baranowsk.** Determination of selected drugs in human urine by differential pulse voltammetry technique. *Bioelectrochemistry.* 2008, Vol. 1, 73, pp. 5-10.

88. **T.M. Oliveira, F.W. Ribeiro, J.E. Soares, P.de Lima-Neto, A.N. Correia.** Square-wave adsorptive voltammetry of dexamethasone: redox mechanism, kinetic properties, and electroanalytical determinations in multicomponent formulations. *Analytical Biochemistry.* 2011, 413, pp. 148-156.

APPENDIX

Drug Release

Standard Calibration Curve of DEX

Standard curve was made by preparing DEX solution in several concentrations; such as 0.1, 0.2, 0.3, 0.5, 1.5, 2, 5, 8, 10 µg/mL in PBS solution. The absorbance was observed with UV-Vis spectroscopy and noted as follows:

Table A1 - Absorbance of DEX solution in PBS

DEX µg/ml	Absorbance
0	0
0.1	0.002
0.2	0.004
0.3	0.010
0.5	0.021
1.5	0.063
2	0.075
5	0.200
8	0.320
10	0.409

From the absorbance data written above, curve was built and line equation was made, as shown in the figure below:

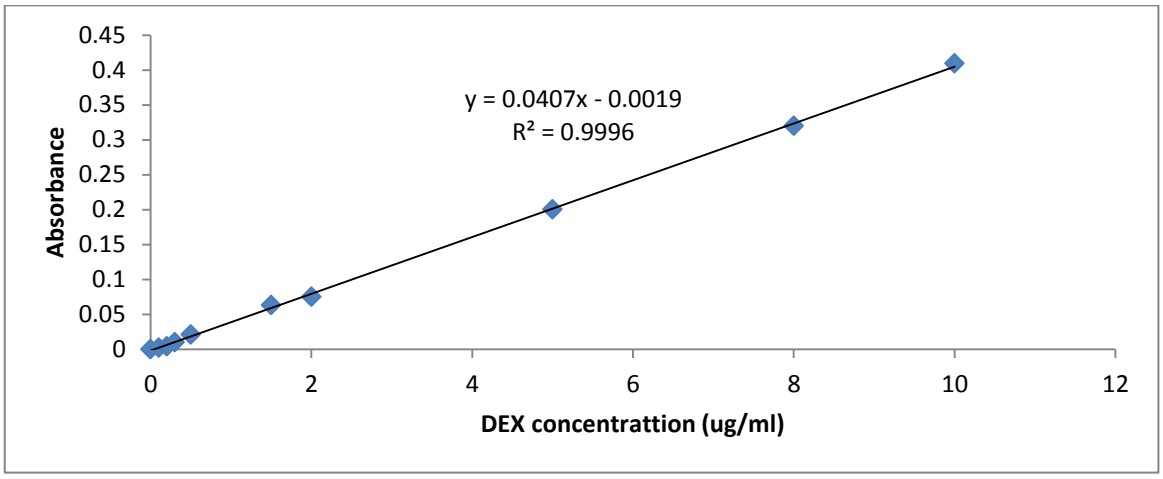

Figure A1 - Standard calibration curve for DEX solution in PBS

Based on the linear equation above, for one known absorbance (from UV-Vis spectroscopy), the concentration can be calculated as follows:

$$x = \frac{y + 0.0019}{0.0407}$$

Drug release calculation:

$$c_{n-concentration\ of\ Dex\ \ in\ n\ aliquot.}$$

$$m_n - mass\ of\ released\ Dex\ (\mu g)\ in\ n\ aliquot.$$

$$M\ - mass\ of\ Dex\ (\mu g)\ in\ immersed\ granules.$$

$$For\ HAP + DEX: in\ 22{,}3mg\ of\ granules\ M(DEX) = 2{,}03mg$$

$$Drug\ released\ (\%) = \frac{m_n}{M} \cdot 100\%$$

$$m_1 = 200 \cdot c_1$$

$$m_2 = 200 \cdot c_2 + 4 \cdot c_1$$

$$m_3 = 200 \cdot c_3 + 4 \cdot c_2 + 4 \cdot c_1$$

$$m_n = 200 \cdot c_n + 4 \cdot c_{n-1} + \cdots + 4 \cdot c_1$$

Table A2 – Drug release (HAP+DEX)

Time (min)	Absorbance	Dex Concentration in PBS(µg/ml)	Drug released (µg)	Drug released %
0	0	0	0	0
30	0.065	1.644	328.595	16.21
45	0.083	2.086	423.622	20.90
65	0.104	2.602	535.160	26.40
90	0.126	3.143	653.676	32.25
120	0.166	4.125	862.806	42.56
150	0.169	4.199	894.049	44.11
180	0.188	4.666	1004.212	49.54
240	0.193	4.789	1047.445	51.67
370	0.231	5.722	1253.332	61.83
1260	0.280	6.926	1517.008	74.84
1440	0.303	7.491	1657.735	81.78
1800	0.283	7.000	1589.420	78.41
4020	0.320	7.909	1799.239	88.76
4320	0.328	8.106	1870.187	92.26
5700	0.327	8.081	1897.696	93.62
7050	0.342	8.450	2003.730	98.85
7440	0.332	8.204	1988.388	98.09
8460	0.327	8.081	1996.634	98.50
8835	0.319	7.885	1989.646	98.15
9960	0.309	7.639	1972.045	97.29
10260	0.313	7.737	2022.256	99.76
11400	0.287	7.098	1925.440	94.98
11760	0.280	6.926	1919.435	94.69
12900	0.289	7.147	1991.366	98.23